**FUNDAÇÃO GETULIO VARGAS**
**SCHOOL OF APPLIED MATHEMATICS**

**RAPHAEL FELBERG LEVY**

# UTILIZATION OF ENVIRONMENTAL AND EPIDEMIOLOGICAL INDICATORS IN THE STUDY OF MALARIA DYNAMICS

Rio de Janeiro
2023

**RAPHAEL FELBERG LEVY**

# UTILIZATION OF ENVIRONMENTAL AND EPIDEMIOLOGICAL INDICATORS IN THE STUDY OF MALARIA DYNAMICS

Bachelor dissertation presented to the School of Applied Mathematics (FGV/EMAp) to obtain the Bachelor's degree in Applied Mathematics.

Area of Study: Biological modeling.

Advisor: Flávio Codeço Coelho

Rio de Janeiro

2023

**RAPHAEL FELBERG LEVY**

# UTILIZATION OF ENVIRONMENTAL AND EPIDEMIOLOGICAL INDICATORS IN THE STUDY OF MALARIA DYNAMICS

Bachelor dissertation presented to the School of Applied Mathematics (FGV/EMAp) to obtain the Bachelor's degree in Applied Mathematics.

Area of Study: Biological modeling.

And approved in 12/12/2023

---

Flávio Codeço Coelho
School of Applied Mathematics

---

Claudio José Struchiner
School of Applied Mathematics

---

Mônica da Silva-Nunes
Universidade Federal de São Carlos - UFSCar

# Acknowledgements

To my family, especially my parents, for all the support and encouragement throughout not only my undergraduate studies but also throughout the entire journey up to this moment.

To my supervisor, Flávio Codeço Coelho, for being my guide in the development of this work and for introducing me to the field of modeling biological phenomena.

To all the professors I had the opportunity to meet and from whom I had the pleasure of learning during my undergraduate studies, and to the teaching assistants who were willing to help in the most challenging moments.

Finally, I would like to express my gratitude to all my friends who accompanied and supported me until now. The last 4 years wouldn't have been the same without you.

# Abstract

Malaria is an infectious disease transmitted by mosquitoes infected by protozoa of the genus *Plasmodium*, with the Amazon region being considered an endemic area for the disease. This work aims to analyze the behavior of this transmission based on climatic and environmental changes, such as temperature, precipitation and deforestation, through proposed modifications to the SIR and SEI models, in order to contribute to the study of applications of external effects on the evolution of the disease. The Trajetórias Project, developed by the Synthesis Center on Biodiversity and Ecosystem Services (SinBiose/CNPq) will be used as a reference base for the analyses.

Keywords: Biological modelling. Malaria. Amazon. SIR. SEI.

# Resumo

A malária é uma doença infecciosa transmitida por mosquitos infectados por protozoários do gênero *Plasmodium*, sendo a região amazônica considerada área endêmica para a doença. Esse trabalho tem como intuito analisar o comportamento dessa transmissão baseado em modificações climáticas e ambientais, como temperatura, precipitação e desmatamento, através de modificações propostas aos modelos SIR e SEI, de forma a contribuir no estudo de aplicações de efeitos externos na evolução da doença. O Projeto Trajetórias, desenvolvido pelo Centro de Biodiversidade e Serviços Ecossistêmicos (SinBiose/CNPq), será usado como base de referência para as análises.

Palavras-chave: Modelagem biológica. Malária. Amazônia. SIR. SEI.

# List of Figures

# List of Tables

# Contents

# 1 Introduction

The Amazon is one of the largest and most biodiverse tropical forests in the world, harboring numerous species of plants, animals, and microorganisms, including vectors and pathogens responsible for the transmission of various diseases. Among them, one of the most common is malaria, caused by protozoa of the genus *Plasmodium*, transmitted by the bite of the infected female mosquito of the genus *Anopheles*. It is present in 22 American countries, but the areas with the highest risk of infection are located in the Amazon region, encompassing nine countries, which accounted for 68% of infection cases in 2011 (PIMENTA et al., 2015). Although malaria is prevalent in the Americas, it is not limited to this continent and is found in countries in Africa and Asia, resulting in more than two million cases of infection and 445,000 deaths worldwide in 2016 (JOSLING; WILLIAMSON; LLINÁS, 2018).

Notably, vector-borne disease transmission is closely related to environmental changes that interfere with the ecosystem of both transmitting organisms and affected organisms. In the case of the Amazon, agricultural and livestock settlements are among the factors that most favor disease transmission, both due to the deforestation they cause for establishment and the clustering of people in environments close to the vector's habitat (SILVA-NUNES, M. da et al., 2008), especially by clustering non-immune migrants near these natural and artificial breeding sites (SILVA-NUNES, Mônica da et al., 2012).

Additionally, other factors such as rainfall, wildfires, and mining also significantly influence disease transmission in the region. These events result in habitat loss, ecosystem fragmentation, and climate changes, affecting the distribution and abundance of vectors and hosts, as well as their interaction with pathogens. Furthermore, population growth and urbanization also play a crucial role in disease spread, increasing human exposure to vectors and infection risks.

In this context, this work aims to investigate vector-borne disease transmission in the Amazon and analyze how environmental impacts influence the dynamics of malaria transmission, the ecological and socioeconomic factors affecting this spread, and possible prevention and control strategies. The main reference for this research is the Trajetórias Project, developed by the Center for Biodiversity and Ecosystem Services (SinBiose/CNPq), which is a dataset including environmental, epidemiological, economic, and socioeconomic indicators for all municipalities in the Legal Amazon, analyzing the spatial and temporal relationship between economic trajectories linked to the dynamics of agrarian systems, whether they are family-based rural or large-scale agricultural and livestock production, the availability

of natural resources, and the risk of diseases (RORATO et al., 2023).

# 2 Metodology

For the elaboration of the work, population data from the Trajetórias Project dataset and climatic data from the Climate Data will be used. Methods of disease transmission based on ordinary differential equations, such as the SIR model, will be addressed. Starting with a simple modeling approach, environmental phenomena such as deforestation and burning will be included to assess how modifications in the ecosystem will interfere with the previously developed model. Computational calculations were performed using the SageMath 9.2 environment, utilizing Scipy's numerical integration functions to solve the method.

First I will be describing SIR (COELHO, n.d.; PRASAD et al., 2022), which can be considered the foundation of the models that will be used throughout the project. Developed by W. O. Kermack and A. G. McKendrick in 1927, SIR is one of the most widely used models for epidemic modeling, considering three compartments:

$S$ : number of susceptible individuals

$I$ : number of infected individuals

$R$ : number of recovered individuals

In this model, healthy individuals in the $S$ class are susceptible to contact with individuals in the $I$ class and are transferred to this compartment if they contract the disease. Infected individuals can spread the disease through direct contact with susceptible individuals, but they can also become immune over time and are transferred to the $R$ compartment. In general, $R$ includes the total of recovered (immune) individuals and those who died from the disease, but we can assume that the number of deaths is very low compared to the total population size and can be ignored. We also assume that individuals in this category will not revert to being susceptible or infectious.

Considering an epidemic over a short period and that the disease is not fatal, we can ignore vital dynamics of birth and death. With this, we can describe the SIR model through the following system of ordinary differential equations (ODEs):

$$\begin{cases} \dfrac{dS}{dt} = -\dfrac{\beta SI}{N} \\ \dfrac{dI}{dt} = \dfrac{\beta SI}{N} - \gamma I \\ \dfrac{dR}{dt} = \gamma I \end{cases}$$

In the model, $N(t) = S(t) + I(t) + R(t)$, i.e., the total population at time $t$, while $\beta$ is the infection rate, and $\gamma$ is the recovery rate. Given that $S + I + R$ is always constant if we ignore birth and death, we have $\dfrac{dS}{dt} + \dfrac{dI}{dt} + \dfrac{dR}{dt} = 0$.

For the disease to spread, it is easy to see that $\dfrac{dI}{dt} = \dfrac{\beta SI}{N} - \gamma I > 0$. Thus, $\dfrac{\beta SI}{N} > \gamma I \Rightarrow \dfrac{\beta S}{N} > \gamma$. Assuming we are at the beginning of the infection, given that we want to observe its spread, $I$ will be very small, and $S \approx N$. We then conclude that $\dfrac{\beta N}{N} > \gamma \Rightarrow \dfrac{\beta}{\gamma} > 1$. This dimensionless value can be derived by nondimensionalizing the model: let $y^* = \dfrac{S}{N}$, $x^* = \dfrac{I}{N}$, $z^* = \dfrac{R}{N}$, and $t^* = \dfrac{t}{1/\gamma} = \gamma t$, so that $y^* + x^* + z^* = 1$. Substituting the system of ODEs above using these values:

$$\begin{cases} \dfrac{dS}{dt} = \dfrac{d(y^*N)}{d(t^*/\gamma)} = -\dfrac{\beta SI}{N} = -\dfrac{\beta(y^*N)(x^*N)}{N} = -\beta y^* N x^* \\ \dfrac{dI}{dt} = \dfrac{d(x^*N)}{d(t^*/\gamma)} = \dfrac{\beta SI}{N} - \gamma I = \dfrac{\beta(y^*N)(x^*N)}{N} - \gamma(x^*N) = \beta y^* N x^* - \gamma x^* N \\ \dfrac{dR}{dt} = \dfrac{d(z^*N)}{d(t^*/\gamma)} = \gamma I = \gamma(x^*N) \end{cases}$$

Now, canceling the factors $N$ and $\gamma$ on both sides of the equations:

$$\begin{cases} \dfrac{d(y^*)}{d(t^*)} = -\dfrac{\beta y^* x^*}{\gamma} \\ \dfrac{d(x^*)}{d(t^*)} = \dfrac{\beta y^* x^*}{\gamma} - x^* \\ \dfrac{d(z^*)}{d(t^*)} = x^* \end{cases}$$

Thus, we have a system given only by $y^*$ and $x^*$ and the parameter $\frac{\beta}{\gamma}$, which we can call $R_0$.

As this work will be primarily focused on malaria modeling, I will now present one of the first models developed specifically for this disease, by Sir Ronald Ross in 1911 (BACAËR, 2011), which uses two distinct ordinary differential equations (ODEs) different from those presented above:

$$\begin{cases} \frac{dI}{dt} = bp'i\frac{N-I}{N} - aI \\ \\ \frac{di}{dt} = bp(n-i)\frac{I}{N} - mI \end{cases}$$

In this case, $N$ is the total human population, $I(t)$ is the number of infected humans at time $t$, $n$ is the total mosquito population, $i(t)$ is the number of infected mosquitoes at time $t$, $b$ is the biting rate, $p$ is the probability of transmission from human to mosquito per bite, $p'$ is the probability of transmission from mosquito to human per bite, $a$ is the recovery rate of human infection, and $m$ is the mosquito mortality rate. $bp'ii\frac{N-I}{N}dt - aIdt$ represent, respectively, the number of new infected humans and the number of recovered humans in the interval $dt$, while $bp(n-i)\frac{I}{N}dt - mIdt$ represent, respectively, the number of new infected mosquitoes and the number of mosquitoes that die in that time interval, assuming that infection does not affect the mosquito mortality rate.

For this model, Ross discussed two equilibrium points, where $\frac{dI}{dt} = \frac{di}{dt} = 0$. They occur when $I = i = 0$, which is the case where there is no malaria, and, for $I, i > 0$, $I = N\frac{1 - amN/(b^2pp'n)}{1 + aN/(bp'n)}$ and $i = n\frac{1 - amN/(b^2pp'n)}{1 + m/(bp)}$. Furthermore, for the disease to establish itself, $n$ must be greater than a threshold value $n^* = \frac{amN}{b^2pp'}$. In this case, the disease becomes endemic. If $n < n^*$, the equilibrium will be at $I = i = 0$, and the disease will disappear.

Dividing the equations of the equilibrium points by $I \times i$, we have:

$$\begin{cases} \frac{bp}{N} = \frac{bpn}{Ni} - \frac{m}{I} \\ \\ \frac{bp'}{N} = \frac{bp'}{I} - \frac{a}{i} \end{cases}$$

Which transforms the problem into a linear system with two unknowns, $I$ and $i$.

Now, I will present the model that will be used for the development of the work, based on the one developed by Paul E. Parham and Edwin Michael in 2010, which takes into account factors such as rainfall and temperature ($R$ and $T$, respectively) (PARHAM; MICHAEL, 2010).

Defining the equations that will be used:

$$\begin{cases} \dfrac{dS_H}{dt} = -ab_2\left(\dfrac{I_M}{N}\right)S_H \\ \dfrac{dI_H}{dt} = ab_2\left(\dfrac{I_M}{N}\right)S_H - \gamma I_H \\ \dfrac{dR_H}{dt} = \gamma I_H \\ \dfrac{dS_M}{dt} = b - ab_1\left(\dfrac{I_H}{N}\right)S_M - \mu S_M \\ \dfrac{dE_M}{dt} = ab_1\left(\dfrac{I_H}{N}\right)S_M - \mu E_M - ab_1\left(\dfrac{I_H}{N}\right)S_M l(\tau_M) \\ \dfrac{dI_M}{dt} = ab_1\left(\dfrac{I_H}{N}\right)S_M l(\tau_M) - \mu I_M \end{cases}$$

It is necessary to mention that the original model used $I_M(t-\tau)$ in $\dfrac{dI_H}{dt}$ and $I_H(t-\tau)$ in $\dfrac{dE_M}{dt}$ (in the transition from $E$ to $I$) and $\dfrac{dI_M}{dt}$, respectively. However, as this would make the model based on delay differential equations, it was recommended by the advisor to disregard this difference and use only the current time $t$.

Having the model equations for the human and mosquito populations, I will first define the parameters used in the modeling and other necessary functions, and then the variables used:

| **Parameter** | **Definition** | **Formula** |
|---|---|---|
| $T(t)$ | Temperature | $T_1(1 + T_2 \cos(\omega_1 t - \phi_1))$ |
| $R(t)$ | Precipitation | $R_1(1 + R_2 \cos(\omega_2 t - \phi_2))$ |
| $b(R, T)$ | Mosquito birth rate (/ day) | $\frac{B_E p_E(R) p_L(R,T) p_P(R)}{(\tau_E + \tau_L(T) + \tau_P)}$ |
| $a(T)$ | Biting rate (/day) | $\frac{(T - T_1)}{D_1}$ |
| $\mu(T)$ | Mosquito mortality rate per capita (/ day) | $-\log(p(T))$ |
| $\tau_M(T)$ | Duration of the sporozoite cycle (days) | $\frac{DD}{(T - T_{min})}$ |
| $\tau_L(T)$ | Duration of larval development phase (days) | $\frac{1}{c_1 T + c_2}$ |
| $p(T)$ | Daily mosquito survival rate | $e^{(-1/(AT^2+BT+C))}$ |
| $p_L(R)$ | Probability of larval survival dependent on rainfall | $(\frac{4p_{ML}}{R_L^2})R(R_L - R)$ |
| $p_L(T)$ | Probability of larval survival dependent on temperature | $e^{-(c_1 T + c_2)}$ |
| $p_L(R, T)$ | Probability of larval survival dependent on temperature and rainfall | $p_L(R) p_L(T)$ |
| $l(\tau_M)(T)$ | Probability of mosquito survival during the sporozoite cycle (/ day) | $p(T)^{\tau_M(T)}$ |
| $M(t)$ | Total number of mosquitoes | $S_M(t) + E_M(t) + I_M(t)$ |
| $N(t)$ | Total number of humans | $S_H(t) + I_H(t) + R_H(t)$ |

Table 1 – Parameters used in the modeling

| **Parameter** | **Definition** |
|---|---|
| $b_1$ | Proportion of bites from susceptible mosquitoes on infected humans that result in infection |
| $b_2$ | Proportion of bites from infected mosquitoes on susceptible humans that result in infection |
| $\gamma$ | 1/Average duration of infectiousness in humans (days$^{-1}$) |
| $T_1$ | Mean temperature in the absence of seasonality ($^{\circ}C$) |
| $T_2$ | Amplitude of seasonal variability in temperature |
| $R_1$ | Average monthly precipitation in the absence of seasonality (mm) |
| $R_2$ | Amplitude of seasonal variability in precipitation |
| $\omega_1$ | Angular frequency of seasonal oscillations in temperature (months$^{-1}$) |
| $\omega_2$ | Angular frequency of seasonal oscillations in precipitation (months$^{-1}$) |
| $\phi_1$ | Phase lag of temperature variability (phase shift) |
| $\phi_2$ | Phase lag of precipitation variability (phase shift) |
| $B_E$ | Number of eggs laid per adult per oviposition |
| $p_{ME}$ | Maximum probability of egg survival |
| $p_{ML}$ | Maximum probability of larval survival |
| $p_{MP}$ | Maximum probability of pupal survival |
| $\tau_E$ | Duration of the egg development phase (days) |
| $b_3^*$ | Infection rate in exposed mosquitoes ($1/\tau_M(T)$) |

Table 2 – Parameters used in the modeling

| **Parameter** | **Definition** |
|---|---|
| $\tau_P$ | Duration of the pupal development phase (days) |
| $R_L$ | Rainfall threshold until breeding sites are eliminated, removing immature individuals (mm) |
| $T_{min}$ | Minimum temperature, below which there is no development of the parasite: 14.5 ($^\circ C$) |
| $DD$ | Degree-days for parasite development. Number of degrees by which the daily average temperature exceeds the minimum development temperature. "Sum of heat" for maturation: 105 ($^\circ C$ days) |
| $A$ | Empirical sensitivity parameter ($^\circ C^2$ days)$^{-1}$ |
| $B$ | Empirical sensitivity parameter ($^\circ C$ days)$^{-1}$ |
| $C$ | Empirical sensitivity parameter (days$^{-1}$) |
| $D_1$ | Constant: 36.5 ($^\circ C$ days) |
| $c_1$ | Empirical sensitivity parameter ($^\circ C$ days)$^{-1}$ |
| $c_2$ | Empirical sensitivity parameter (days$^{-1}$) |
| $T'^*$ | Empirical temperature parameter ($^\circ C$) |

Table 3 – Parameters used in the modeling

Parameters marked with * were added during the development of the modeling to correct inaccuracies derived from the original equations in the reference article. The definition of $DD$ was taken from (MCCORD, 2016) and (DETINOVA; BERTRAM; ORGANIZATION, 1962).

Having the equations and parameters, the modeling was initially done using data from the rural area of Manaus, in the period between 2004 to 2008, which were selected due to the higher incidence of malaria cases caused by *P. vivax*, the species responsible for the highest number of cases in Brazil (OLIVEIRA-FERREIRA et al., 2010; CODEÇO et al., 2021). Using the incidence function used in the Trajetorias project (RORATO et al., 2023), we have:

$$\text{Inc}(d, m, z, t_1, t_2) = \frac{\text{Cases}(d, m, z, t_1, t_2)}{\text{Pop}(m, z, (t_1 + t_2)/2) \times 5 \text{ years}} \times 10^5,$$

where $\text{Cases}(d, m, z, t_1, t_2)$ is the number of cases of disease $d$ in zone $z$ of municipality $m$,

and $t_1$ and $t_2$ are the initial and final years of the interval, while $\text{Pop}(m, z, (t_1 + t_2)/2) \times 5$ years is the population in zone $z$ of municipality $m$ in the middle of the period multiplied by the total number of observation years. In this case, we could indicate as:

$$\text{Inc}(\text{Vivax, Manaus, Rural}, 2004, 2008) = \frac{\text{Cases}(\text{Vivax, Manaus, Rural}, 2004, 2008)}{\text{Pop}(\text{Manaus, Rural}, 2006) \times 5 \text{ years}} \times 10^5$$

$$184030.8 = \frac{78745}{5\text{Pop}} \times 10^5 \Rightarrow Pop \approx 8558$$

Using data on the total population of Manaus in this period, with an incidence of 3106.4 and a number of cases of 262264, the total population of the municipality was estimated to be 1688540 inhabitants. Thus, the rural population could be considered as approximately 0.5% of the municipality's population.

Having estimated the percentage size of the rural population in the city, it was possible to calculate this population for each of the years of the analysis through linear interpolation using historical series data from IBGE (IBGE, n.d.):

| **Year** | **Estimated rural population** |
|---|---|
| 2004 | 7717 |
| 2005 | 7889 |
| 2006 | 8061 |
| 2007 | 8233 |
| 2008 | 8492 |
| 2009 | 8751 |

Table 4 – Manaus' rural population from 2004 to 2009

As there were population data for the years 2000, 2007, and 2010, interpolations were performed with different initial and final points, using data from 2000 to 2007 for 2004-2007 and from 2007 to 2010 for 2008-2009, ensuring the correct use of the 2007 population.

Now, describing a bit of the theory behind environmental factors, according to (NORRIS, 2004), the removal of tree canopies allowed the resurgence of malaria in South America. In deforested areas, without tree canopies covering the ground, water puddles under sunlight

attract mosquitoes of the species *Anopheles darlingi*, the main vector related to human malaria in the Amazon (RONDÔNIA, n.d.). They are usually less commonly found in still intact forests. This is because light and heat favor the development of larvae and pupae, in addition to a greater availability of algae for larval feeding (SILVA-NUNES, 2010). The increase in ambient temperature also favors the vectorial capacity of mosquitoes. Deforestation also attracts and brings humans closer to take part in logging, agriculture, and road construction activities, bringing individuals infected with *Plasmodium* to an area where both the vector and the environment have already been modified to favor transmission. Furthermore, agriculture also promotes river sedimentation, providing suitable environments for breeding sites. Therefore, it can be considered a relevant change for the model to take into account deforestation, the increase in survival probabilities of eggs, larvae, and pupae, as well as increasing the proportion of bites that lead to infection, due to the increased human population density in areas near mosquito breeding sites.

# 3 Results

Analyzing the results obtained with the original parameters from the article by Parham and Michael ($T' = 19.9$ (also called $T_1$ in the article), $T_1 = 23.2$, $T_2 = 0.07$, $\omega_1 = 0.67$, $\phi_1 = 1.53$, $R_1 = 85.9$, $R_2 = 0.98$, $\omega_2 = 0.65$, $\phi_2 = 1.99$, $A = -0.03$, $B = 1.31$, $C = -4.4$, $b_1 = 0.04$, $b_2 = 0.09$, $T_{min} = 14.5$, $\gamma = 1/120$, $R_L = 50$, $c_1 = 0.00554$, $c_2 = -0.06737$ (PARHAM; MICHAEL, 2010), (OKUNEYE; GUMEL, 2017)), and using the previously estimated average population and an arbitrary value for the mosquito population, of 10000, assuming 1000 infected humans and 5000 exposed mosquitoes at $t = 0$, the modeling is as follows [1]:

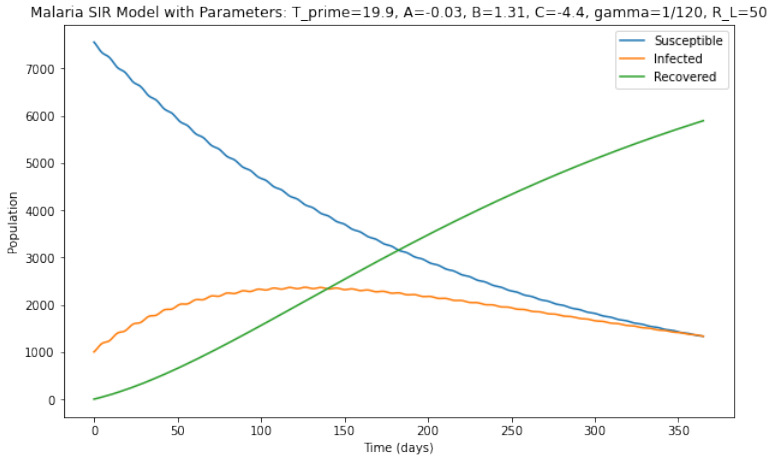


Figure 1 – SIR with original parameters

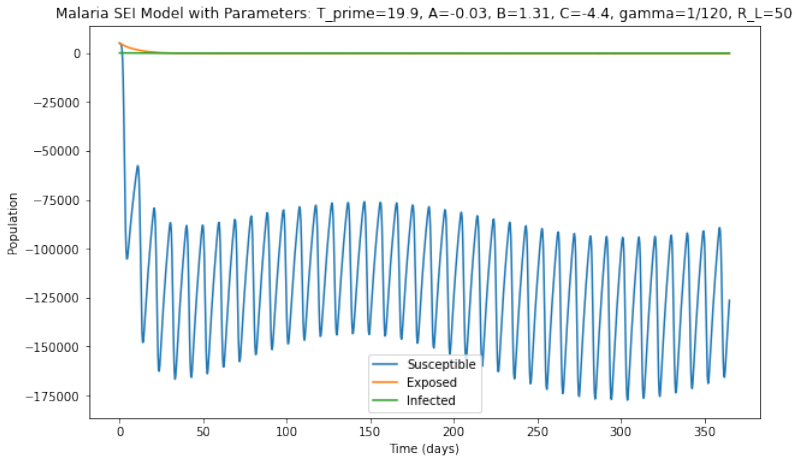


Figure 2 – SEI with original parameters

[1] The development of the model with the original data can be found at https://github.com/RaphaLevy/Undergraduate_Dissertation/blob/main/modeling_files/Original_Parameters.ipynb.

With this initial modeling, a strong oscillation in the number of susceptible humans and mosquitoes, as well as infected humans, is noticeable. Furthermore, it is evident that with these parameters, the disease will not become endemic, as the number of infected humans tends to 0 throughout the year, while the population of susceptible mosquitoes becomes negative, and the population of exposed and infected individuals also tends to 0. These effects were characterized by temperature and precipitation oscillating in very short periods of time, attributed to a high value of $\omega$ for both functions.

Starting with only a single infected human and exposed mosquito, the oscilatting population isn't noticeable in the SIR plot, however the mosquito population still becomes negative.

Now, the first necessary modification is to correct the temperature and precipitation to consider data from Manaus, as the original paper uses data from Tanzania. So, collecting climatological data from Manaus from (CLIMATEDATA.ORG, n.d.), the average temperature and precipitation were estimated as 26.4 $°C$ and 250.083 mm, respectively. With this data, the amplitude of seasonal variability, angular frequency, and phase lag of variability for both were defined to approximate the real values:

| **Parameter** | **Value** |
|---|---|
| $T_1$ | $26.4°C$ |
| $T_2$ | 0.025 |
| $\omega_1$ | 0.017 $(\text{months})^{-1}$ |
| $\phi_1$ | -1.45 |
| $R_1$ | 250.083 mm |
| $R_2$ | 0.565 |
| $\omega_2$ | 0.02 $(\text{months})^{-1}$ |
| $\phi_2$ | 1.6 |

Table 5 – Values for climatic parameters

The amplitude parameters ($T_2$ and $R_2$) and phase lag parameters ($\phi_1$ and $\phi_2$) are dimensionless. The temperature and precipitation throughout the year then evolve as

follows [2]:

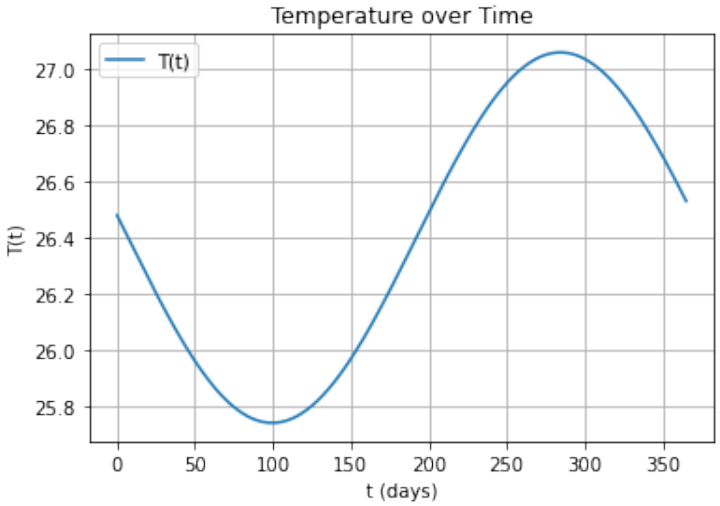


Figure 3 – Temperature graph

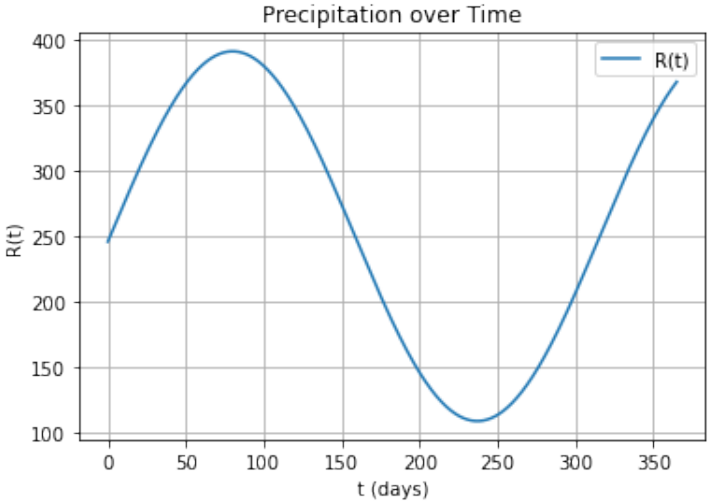


Figure 4 – Precipitation graph

In order to ensure the correctness of the function with the parameters used, I calculated the temperature values for the months of October and May, which are the hottest and coldest months of the year with average temperatures of 27.6 $°C$ and 25.8 $°C$, respectively. Additionally, I calculated the precipitation values in March and August, which are the months with the highest and lowest precipitation, with 395 mm and 114 mm, respectively. The obtained average values were 27.06 $°C$, 25.86 $°C$, 390.67 mm, and 112.89 mm.

With the temperature and precipitation parameters ready for an initial analysis, the

[2] The development of the model with the original data can be found at https://github.com/RaphaLevy/Undergraduate_Dissertation/blob/main/modeling_files/Adapting_T_and_R.ipynb.

evolution of human and mosquito populations was verified. The results can be found in Appendices 1 and 2 [3].

Notably, this result is still incorrect, as the mosquito population still becomes negative over time. However, the daily oscillations was indeed eliminated, due to the modifications made to $\omega_1$ and $\omega_2$. Another parameter that should also be adapted in consideration for our new climatic values was $R_L$, the rainfall limit beyond which breeding sites get flushed out and no immature stages survive. In the original paper, $R_L$ was defined as 50 mm, which is too low for the high precipitation in the Amazon, which has a maximum of almost 400 mm in March. Because of this, I increased $R_L$ from 50 mm to 450 mm. The results can be found in Appendices 3 and 4 [4].

Now, while the mosquito population in non-negative, it rapidly declines and becomes extinct. That is due to the value of $\mu$, the mortality rate of mosquitoes, given by $-\log(e^{(-1/(AT^2+BT+C))})$. For small values of $A$, $B$ and $C$, mostly $A$, $\mu$ becomes "relatively" large, and the mosquito population goes extinct. To fix this, I altered these 3 parameters from the initial values of the article, which had $\mu \approx 0.0027$, to $A = 356.3$, $B = 15$ and $C = -48.78$, which gave a $\mu$ of approximately $4.02133 \times 10^{-6}$, and so the mosquito population is nearly constant throughout the analysis. The results, with $A$, $B$ and $C$ as above, can be found in Appendices 5 and 6 [5].

Now, it is possible to see that the mosquito population in fact remains nearly constant, as there is close to no transference between compartments.

To verify what else could be done to allow the transference of individuals between compartments, given the differential equations of the SEI model and the parameters provided to achieve this goal, the value of $\mu$ becomes very close to 0, as seen above, while $l(\tau_M)$, a probability, becomes very close to 1. Therefore, $\frac{dE_M}{dt}$ also becomes very close to 0, causing the exposed function to be linear, while the mosquito population leaving the susceptible compartment almost simultaneously enters the infected compartment, causing mirrored oscillations of $S$ and $I$. To overcome this effect, it was necessary to modify the use of $b_1$ to only move mosquitoes from compartment $S$ to $E$, requiring the inclusion of a new parameter, $b_3$, to move mosquitoes from compartment $E$ to $I$. This rate is inversely related

[3] The development of the graphs above can be found at https://github.com/RaphaLevy/Undergraduate_Dissertation/b
modeling_files/Adapting_T_and_R.ipynb.

[4] The development of the graphs above can be found at https://github.com/RaphaLevy/Undergraduate_Dissertation/b
modeling_files/Adapting_T_and_R.ipynb.

[5] The development of the graphs above can be found at https://github.com/RaphaLevy/Undergraduate_Dissertation/b
modeling_files/Modifying_Constant_Parameters.ipynb.

to the incubation period, so we define

$$b_3 = \frac{T - T_{min}}{DD}$$

Moreover, the parameter $a(T)$ in the transition from exposed mosquitoes to infected was removed, as no new bites occur in this change from compartment $E$ to $I$.

With these modifications, the differential equations of the SEI model were modified:

$$\begin{cases} \dfrac{dS_M}{dt} = b - ab_1\left(\dfrac{I_H}{N}\right)S_M - \mu S_M \\ \\ \dfrac{dE_M}{dt} = ab_1\left(\dfrac{I_H}{N}\right)S_M - \mu E_M - b_3 E_M l \\ \\ \dfrac{dI_M}{dt} = b_3 E_M l - \mu I_M \end{cases}$$

The results can be seen in Apendices 7 to 10, using $T' = 19.9°C$, as originally used, and $T' = 24.4°C$, which is a value lower than the minimum temperature, close to $25.6°C$. Using $T' = 19.9°C$, the human population remains close to what could be seen in Appendix 5, while the mosquito population is now oscillating, with the number of exposed mosquitoes decreasing to values near 0, while the infected population increases. With $T' = 24.4°C$, the SEI plot is very similar, however the increase of the infected population is less noticeable. In the case of the human population, it can be seen that the disease begins at a later time, and the maximum number of infected individuals is lower than what was seen before [6].

Another necessary modification was to disassociate $l$, the probability of mosquito survival during the sporozoite cycle, from the infection rate of exposed individuals $b_3$.

$$\begin{cases} \dfrac{dS_M}{dt} = b - ab_1\left(\dfrac{I_H}{N}\right)S_M - \mu S_M \\ \\ \dfrac{dE_M}{dt} = ab_1\left(\dfrac{I_H}{N}\right)S_M - \mu E_M - b_3 E_M - l E_M \\ \\ \dfrac{dI_M}{dt} = b_3 E_M - \mu I_M \end{cases}$$

With this alteration, it was noted that both populations didn't reach an equilibrium in the first year of analysis, so extending it to 5 years, the results were as seen in Appendices

[6] The development of the graphs above can be found at https://github.com/RaphaLevy/Undergraduate_Dissertation/b modeling_files/SEI_Exposed_to_Infected.ipynb.

11 to 14 [7].

With the SIR/SEI model now properly corrected, it was possible to proceed with the analyses of deforestation application. To do so, I began by calculating the $\mathcal{R}_0$ for both SIR and SEI, as well as for the coupled model, using the formulation from P. van den Driessche (VAN DEN DRIESSCHE; WATMOUGH, 2002) as a reference:

Firstly, we define $X_s$ as the set of all disease-free states,

$$X_s = \{x \geq 0 | x_i = 0, i = 1, \ldots, m\},$$

where $X = (x_1, \ldots, x_n)^T$, such that $x_i \geq 0$ represents the number of individuals in each compartment, and we assume each function to be continuously differentiable at least twice in each variable ($C^2$).

Now, we rearrange the equations so that the first $m$ equations contain the infected individuals. Let $\mathcal{F}_i(x)$ be the rate of appearance of new infections in compartment $i$, $\mathcal{V}_i^+(x)$ be the rate of individuals entering compartment $i$ by other means, and $\mathcal{V}_i^-(x)$ be the rate of individuals leaving compartment $i$. The disease transmission model consists of non-negative initial conditions together with the following system of equations:

$$\dot{x} = f_i(x) = \mathcal{F}_i(x) - \mathcal{V}_i(x), i = 1, \ldots, n,$$

where $\mathcal{V}_i(x) = \mathcal{V}_i^-(x) - \mathcal{V}_i^+(x)$. We also define $F = \left[\frac{\partial \mathcal{F}_i(x_0)}{\partial x_j}\right]$ and $V = \left[\frac{\partial \mathcal{V}_i(x_0)}{\partial x_j}\right]$, where $x_0$ is a Disease-Free Equilibrium (DFE), and $1 \leq i, j \leq m$.

This is equivalent to the Jacobian of these two matrices, after substituting $x_0$, i.e., $S = 1$. $\mathcal{R}_0$ will be given by $\rho(FV^{-1})$, in other words, it will be the spectral radius of the matrix $FV^{-1}$. With the necessary definitions, we can calculate the $\mathcal{R}_0$ for both models as follows:

- **SIR:** In this case, $m = 1$, and our compartments will be arranged as $[I_H, S_H, R_H]$. Since $\mathcal{R}_0$ is calculated with normalized values, we will multiply the necessary equations by $N$ to remove the denominator. Specifically, for the SIR case, as $R_H$ is not used in any of the equations, we can express it solely in terms of $S$ and $I$. Therefore:

  $$\mathcal{F}_i(x): \text{ rate of appearance of new infected individuals in compartment } i$$

  $$\mathcal{F} = \left[ab_2 I_M S_H\right]$$

  Additionally, we have

  $$\mathcal{V}_i(x)^-: \text{ rate of leaving compartment } i$$

[7] The development of the graphs above can be found at https://github.com/RaphaLevy/Undergraduate_Dissertation/b modeling_files/SEI_Exposed_to_Infected.ipynb.

$$\mathcal{V}_i(x)^+ : \text{ rate of entering compartment } i$$

Thus:

$$\mathcal{V}^- = \begin{bmatrix}\gamma I_H\end{bmatrix}$$

$$\mathcal{V}^+ = \begin{bmatrix}0\end{bmatrix}$$

$$\mathcal{V}_i(x) = \mathcal{V}_i(x)^- - \mathcal{V}_i(x)^+$$

Therefore,

$$\mathcal{V} = \begin{bmatrix}\gamma I_H\end{bmatrix}$$

Hence

$$F = \frac{\partial \mathcal{F}}{\partial I_M} = \begin{bmatrix}ab_2 S_H\end{bmatrix}$$

$$V = \frac{\partial \mathcal{V}}{\partial I_H} = \begin{bmatrix}\gamma\end{bmatrix}$$

At the equilibrium, $[S_H^*, I_H^*] = [1, 0]$, so $F = [ab_2]$, $V = [\gamma]$ and $\mathcal{R}_0 = \left|\frac{ab_2}{\gamma}\right|$.

- **SEI:** In this case, $m = 2$, and our compartments will be arranged as $[E_M, I_M, S_M]$. Again, we multiply the necessary equations by $N$ to remove the denominator. Therefore:

$$\mathcal{F} = \begin{bmatrix} ab_1 I_H S_M \\ 0 \end{bmatrix}$$

$$\mathcal{V}^- = \begin{bmatrix} E_M(\mu + b_3 + l) \\ \mu I_M \end{bmatrix}$$

$$\mathcal{V}^+ = \begin{bmatrix} 0 \\ b_3 E_M \end{bmatrix}$$

$$\mathcal{V}_i(x) = \mathcal{V}_i(x)^- - \mathcal{V}_i(x)^+$$

Thus,

$$\mathcal{V} = \begin{bmatrix} E_M(\mu + b_3 + l) \\ \mu I_M - b_3 E_M \end{bmatrix}$$

Hence

$$F = \frac{\partial \mathcal{F}}{\partial E_M, I_H} = \begin{bmatrix} \frac{\partial ab_1 I_H S_M}{\partial E_M} & \frac{\partial ab_1 I_H S_M}{\partial I_H} \\ \frac{\partial 0}{\partial E_M} & \frac{\partial 0}{\partial I_H} \end{bmatrix} = \begin{bmatrix} 0 & ab_1 S_M \\ 0 & 0 \end{bmatrix}$$

$$V = \frac{\partial \mathcal{V}}{\partial E_M, I_M} = \begin{bmatrix} \frac{\partial E_M(\mu + b_3 + l)}{\partial E_M} & \frac{\partial E_M(\mu + b_3 + l)}{\partial I_M} \\ \frac{\partial \mu I_M - b_3 E_M}{\partial E_M} & \frac{\partial \mu I_M - b_3 E_M}{\partial I_M} \end{bmatrix} = \begin{bmatrix} \mu + b_3 + l & 0 \\ -b_3 & \mu \end{bmatrix}$$

At the equilibrium, $[S_M^*, E_M^*, I_M^*] = [1, 0, 0]$, so

$$F = \begin{bmatrix} 0 & ab_1 \\ 0 & 0 \end{bmatrix},$$

$$V = \begin{bmatrix} \mu + b_3 + l & 0 \\ -b_3 & \mu \end{bmatrix}$$

and $\mathcal{R}_0 = \left| \frac{ab_1 b_3}{(b_3 + l + \mu)\mu} \right|$.

- **SIR/SEI:** In this case, $m = 3$, and our compartments will be arranged as $[I_H, E_M, I_M, S_H, S_M]$. Once again, we multiply the necessary equations by $N$ to remove the denominator. Therefore:

$$\mathcal{F} = \begin{bmatrix} ab_2 I_M S_H \\ ab_1 I_H S_M \\ 0 \end{bmatrix}$$

$$\mathcal{V}^- = \begin{bmatrix} \gamma I_H \\ E_M(\mu + b_3 + l) \\ \mu I_M \end{bmatrix}$$

$$\mathcal{V}^+ = \begin{bmatrix} 0 \\ 0 \\ b_3 E_M \end{bmatrix}$$

$$\mathcal{V}_i(x) = \mathcal{V}_i(x)^- - \mathcal{V}_i(x)^+$$

Thus,

$$\mathcal{V} = \begin{bmatrix} I_H \gamma \\ E_M(\mu + b_3 + l) \\ \mu I_M - b_3 E_M \end{bmatrix}$$

Hence

$$F = \frac{\partial \mathcal{F}}{\partial I_H, E_M, I_M} = \begin{bmatrix} \frac{\partial ab_2 I_M S_H}{\partial I_H} & \frac{\partial ab_2 I_M S_H}{\partial E_M} & \frac{\partial ab_2 I_M S_H}{\partial I_M} \\ \frac{\partial ab_1 I_H S_M}{\partial I_H} & \frac{\partial ab_1 I_H S_M}{\partial E_M} & \frac{\partial ab_1 I_H S_M}{\partial I_M} \\ \frac{\partial 0}{\partial I_H} & \frac{\partial 0}{\partial E_M} & \frac{\partial 0}{\partial I_M} \end{bmatrix} = \begin{bmatrix} 0 & 0 & ab_2 S_H \\ ab_1 S_M & 0 & 0 \\ 0 & 0 & 0 \end{bmatrix}$$

$$V = \frac{\partial \mathcal{V}}{\partial I_H, E_M, I_M} = \begin{bmatrix} \frac{\partial \gamma I_H}{\partial I_H} & \frac{\partial \gamma I_H}{\partial E_M} & \frac{\partial \gamma I_H}{\partial I_M} \\ \frac{\partial E_M(\mu + b_3 + l)}{\partial I_H} & \frac{\partial E_M(\mu + b_3 + l)}{\partial E_M} & \frac{\partial E_M(\mu + b_3 + l)}{\partial I_M} \\ \frac{\partial \mu I_M - b_3 E_M}{\partial I_H} & \frac{\partial \mu I_M - b_3 E_M}{\partial E_M} & \frac{\partial \mu I_M - b_3 E_M}{\partial I_M} \end{bmatrix} =$$

$$\begin{bmatrix} \gamma & 0 & 0 \\ 0 & b_3 + l + \mu & 0 \\ 0 & -b_3 & \mu \end{bmatrix}$$

At the equilibrium, $[S_H^*, S_M^*, I_H^*, E_M^*, I_M^*] = [1, 1, 0, 0, 0]$, so

$$F = \begin{bmatrix} 0 & 0 & ab_2 \\ ab_1 & 0 & 0 \\ 0 & 0 & 0 \end{bmatrix},$$

$$V = \begin{bmatrix} \gamma & 0 & 0 \\ 0 & b_3 + l + \mu & 0 \\ 0 & -b_3 & \mu \end{bmatrix}$$

and $\mathcal{R}_0 = \left| \sqrt{\frac{a^2 b_1 b_2 b_3}{(b_3 + l + \mu)\gamma\mu}} \right| = \sqrt{\mathcal{R}_{0SIR} \times \mathcal{R}_{0SEI}}$.

We can verify that $\mathcal{R}_0$ is indeed dimensionless: $a,\ b_3,\ l,\ \mu$, and $\gamma$ are functions with units of 1/day, while $b_1$ and $b_2$ are dimensionless. Therefore, $\mathcal{R}_0$ for the SIR model has dimensions of (1/day)/(1/day), $\mathcal{R}_0$ for the SEI model has dimensions of $(1/\text{day}^2)/(1/\text{day}^2)$, and the coupled model has dimensions of $(1/\text{day}^3)/(1/\text{day}^3)$.

Before continuing with the modeling, it was decided to analyze the evolution of the rates as a function of temperature and precipitation, instead of time, to see their behavior as $T$ and $R$ vary. In this case, $T'$ was used with value $25.6°C$, in order to approximate $\mathcal{R}_0$ to 0.5, which will be used later in the dissertation. The results can be found starting on Appendix 15 [8].

Now, having the formula for $\mathcal{R}_0$ for the coupled model, the model was executed starting with $E_{M0} = 1$ and $I_{M0} = 1$ and with $E_{M0} = 50000$ and $I_{M0} = 1000$ [9]. With the parameters used in Appendices 13 and 14, $\mathcal{R}_0$ was calculated to be 5.99, which means the disease becomes endemic, as it's value is greater than 1. Using $T' = 25.6°C$ and $A = 12.5$, the results were seen as below:

[8] The development of the graphs above can be found at https://github.com/RaphaLevy/Undergraduate_Dissertation/b
modeling_files/Plotting_Rates.ipynb.

[9] These results can be found respectively at https://github.com/RaphaLevy/Undergraduate_Dissertation/blob/main/
modeling_files/Plotting_with_R0.ipynb and https://github.com/RaphaLevy/Undergraduate_Dissertation/blob/ma
modeling_files/Plotting_with_R0_2.ipynb.

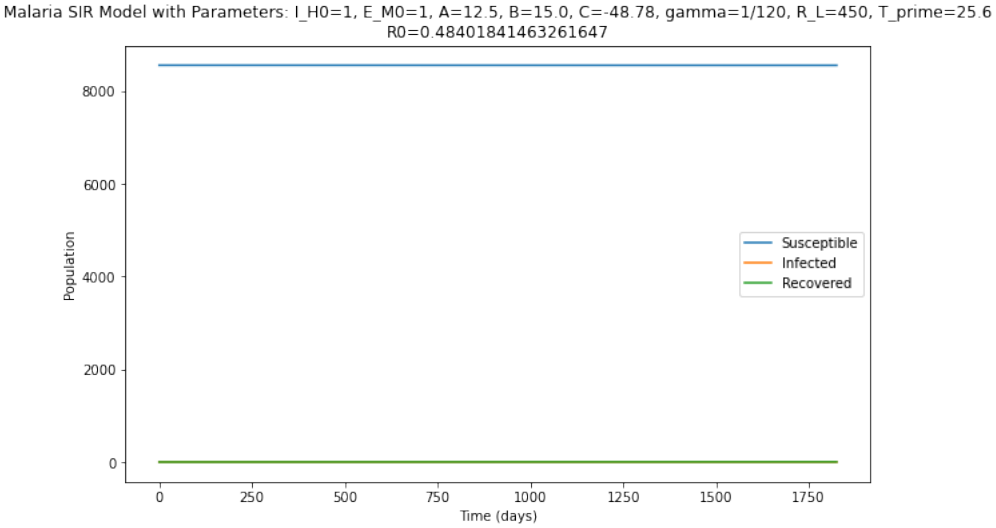


Figure 5 – SIR with $\mathcal{R}_0 < 1$, starting with $E_{M0}$ and $I_{M0} = 1$

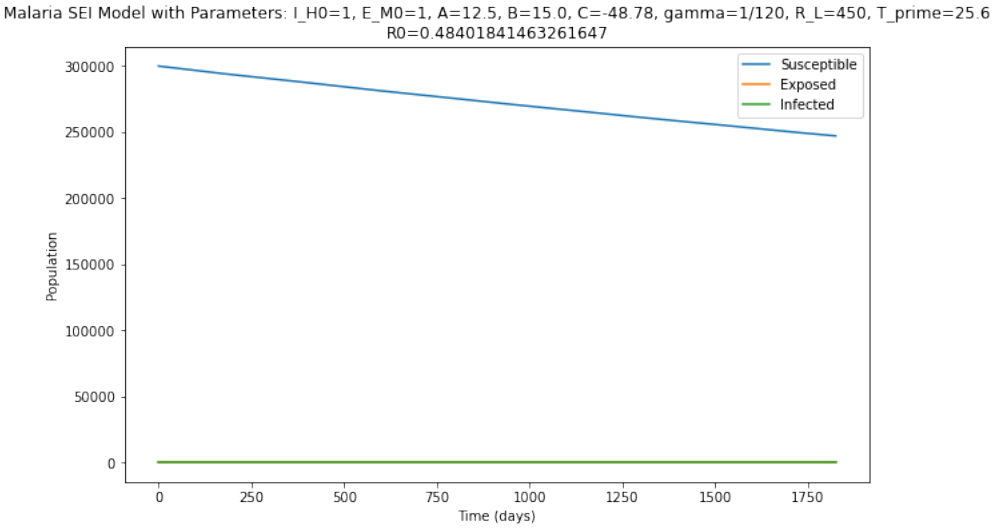


Figure 6 – SEI with $\mathcal{R}_0 < 1$, starting with $E_{M0}$ and $I_{M0} = 1$

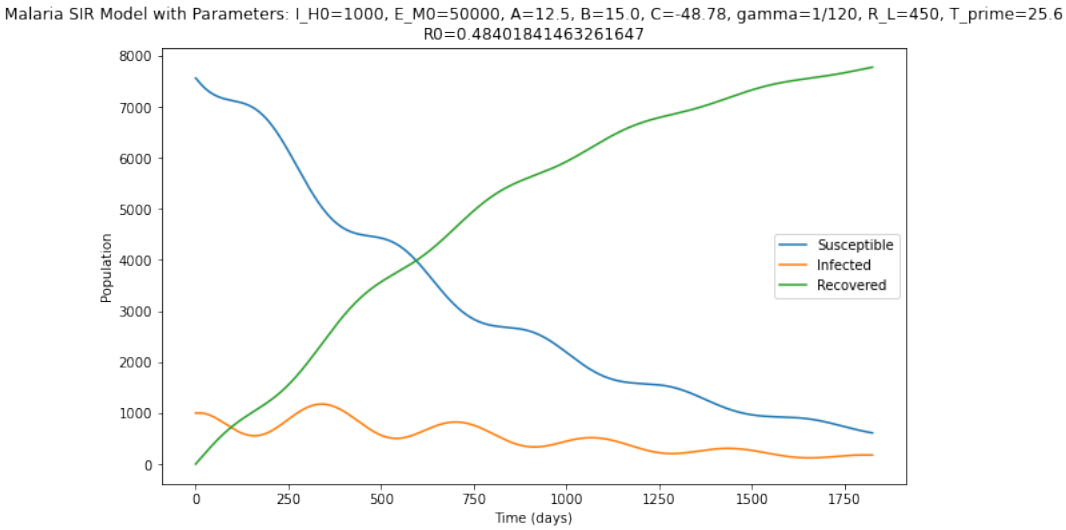


Figure 7 – SIR with $\mathcal{R}_0 < 1$, starting with $E_{M0}$ and $I_{M0} > 1$

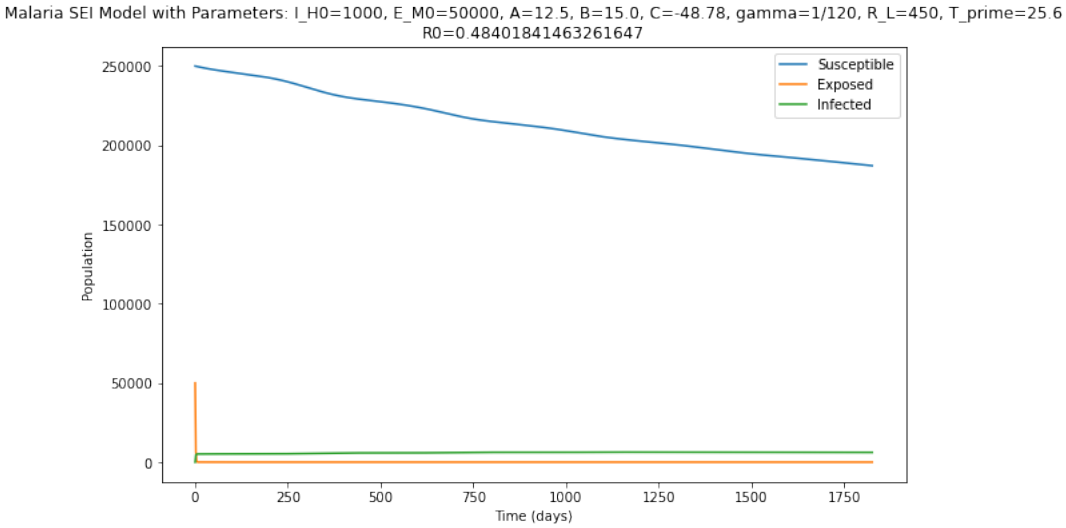


Figure 8 – SEI with $\mathcal{R}_0 < 1$, starting with $E_{M0}$ and $I_{M0} > 1$

With this, as expected, we can see that the disease dies out, specifically the susceptible mosquito population. This would be due to the mortality rate being higher than the birth rate.

Having the model ready, it was possible to proceed with the analysis of the impacts of deforestation. To do that, it was decided to include a multypling factor $k$ for the infection rates of both models, substituting $ab_1$ and $ab_2$ by $kab_1$ and $kab_2$, respectively. This factor will be used to represent the increasing contact between human and mosquito populations due to the the approximation caused by this environmental change. With that in mind, we are interested to see how the disease behaves as $k$ increases, therefore as the contact between the populations increases.

To do this, it was also decided that, instead of using the estimated population of the rural

region of Manaus of 8558, use the population estimated via interpolation for 2004, and include a birth and mortality rate for the human population, $\mu_H$. With the previously obtained values for the human population between 2004 and 2009, the annual birth rate was estimated to be 206.8 births per year. Therefore, this corresponds to approximately 0.56657 births per day and 0.00007 births per day per person, given that the average rural population in Manaus is approximately 8078.5 people between 2004 and 2008. Therefore, using $\mu_h = 0.00007$ and $k$, the final model is given by:

$$\begin{cases} \dfrac{dS_H}{dt} = \mu_H N - akb_2\left(\dfrac{I_M}{N}\right)S_H - \mu_H S_H \\ \dfrac{dI_H}{dt} = akb_2\left(\dfrac{I_M}{N}\right)S_H - \gamma I_H - \mu_H I_H \\ \dfrac{dR_H}{dt} = \gamma I_H - \mu_H R_H \\ \dfrac{dS_M}{dt} = b - akb_1\left(\dfrac{I_H}{N}\right)S_M - \mu S_M \\ \dfrac{dE_M}{dt} = akb_1\left(\dfrac{I_H}{N}\right)S_M - \mu E_M - b_3 E_M - lE_M \\ \dfrac{dI_M}{dt} = b_3 E_M - \mu I_M \end{cases}$$

Where $\mathcal{R}_0$ for SIR is given by $\left|\dfrac{akb_2}{\gamma + \mu_H}\right|$, for SEI is given by $\left|\dfrac{akb_1b_3}{(b_3 + l + \mu)\mu}\right|$ and for the coupled model is given by $\left|\sqrt{\dfrac{a^2k^2b_1b_2b_3}{(b_3 + l + \mu)(\gamma + \mu_H)\mu}}\right|$. It can be immediately seen that $k$ will have a linear impact on $\mathcal{R}_0$.

The results using $k = 1.5,\ 2,\ 2.5,\ 5$ and 10 can be found in Appendices 27 to 36, while plots for each population for multiple values of $k$ can be found in Appendices 37 to 42. The results with $k = 1$ is seen in Figures 5 and 6 [10].

We see that, even starting with a single infected human and exposed mosquito, the disease will eventually become endemic. For $k$ ranging between 1 and 2, $\mathcal{R}_0$ is less than 1, so the disease will die out. However, for $k = 2.5$, $\mathcal{R}_0 > 1$, and it is possible to see, even if only at the end of the analysis, that the disease starts to become endemic, as the human population of infected and recovered have a slight increase by $t = 1500$. For the mosquito

[10] These results can be found respectively at https://github.com/RaphaLevy/Undergraduate_Dissertation/blob/main/modeling_files/Plotting_with_k.ipynb.

population, this behavior is less evident.

For $k = 5$ and $k = 10$, the disease is already endemic, as it is possible to see how it evolves, and that the population will eventually be nearly completely recovered from malaria in the case of the human population. Comparing the results of SIR between $k = 5$ and $k = 10$, the most notable difference is that, the larger the value of $k$, consequently the larger the value of $\mathcal{R}_0$, the faster the disease becomes endemic. For the SEI model, the difference is that the population stabilizes at different ranges. For $k$ up to 2.5, it appears that the disease doesn't become endemic, at least in the first 5 years of the analysis. This may also be due to the large value of $M$, meaning the the exposed and infected mosquito populations are very small relatively to the susceptible population.

For $k = 5$ or 10, the sueceptible population rapidly decreases at a certain point in time, and the infected has a slight increase. In 5 years, the population seems to become stable, however it would be possible to confirm if that's the case by increasing the maximum time of analysis.

Now, we can see that we may double the infection rates, and the disease still won't become endemic. In the image below, it is shown how $\mathcal{R}_0$ increases as $k$ increases:

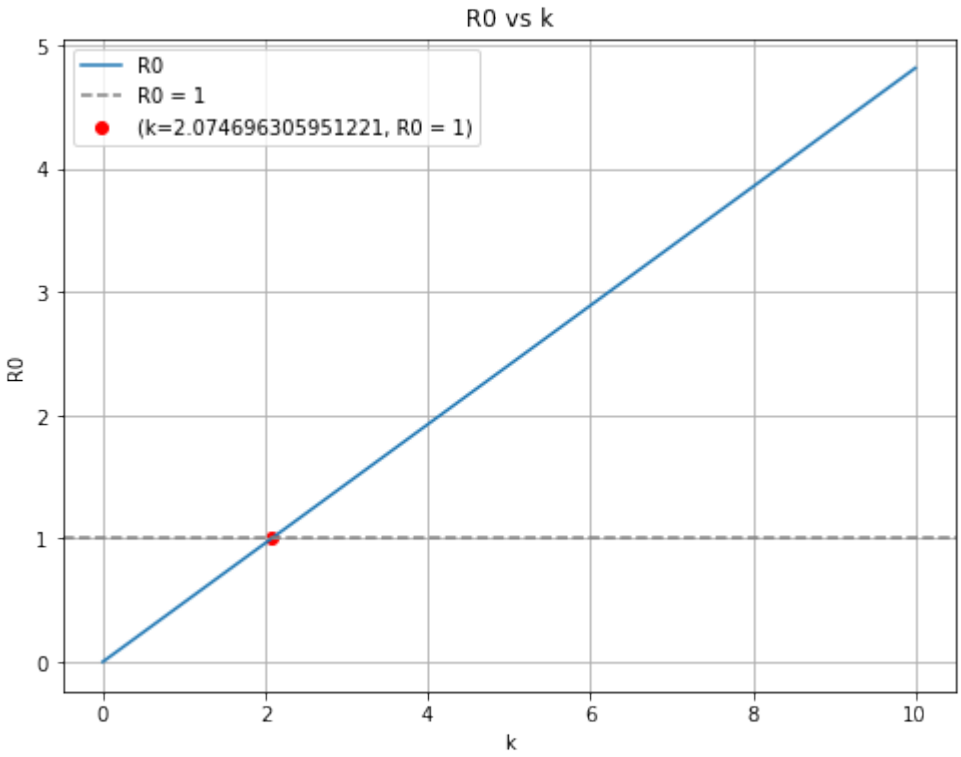


Figure 9 – $\mathcal{R}_0$ given in function of $k$

So, using the parameters from Figures 7 and 8, we can see how the disease will only become endemic when $k > 2.075$. Using this results, we can see that deforestation does indeed cause a significant impact on the disease, as increasing the biting rate in up to 5 to 10 times, starting with a single infected/exposed individual will lead the disease to infect a large portion of the human population, nearly 40%, before decreasing into a stable recovered population.

In fact, we may analyze how the equilibriums of $S_H$ and $I_H$ are affected in function of $k$:

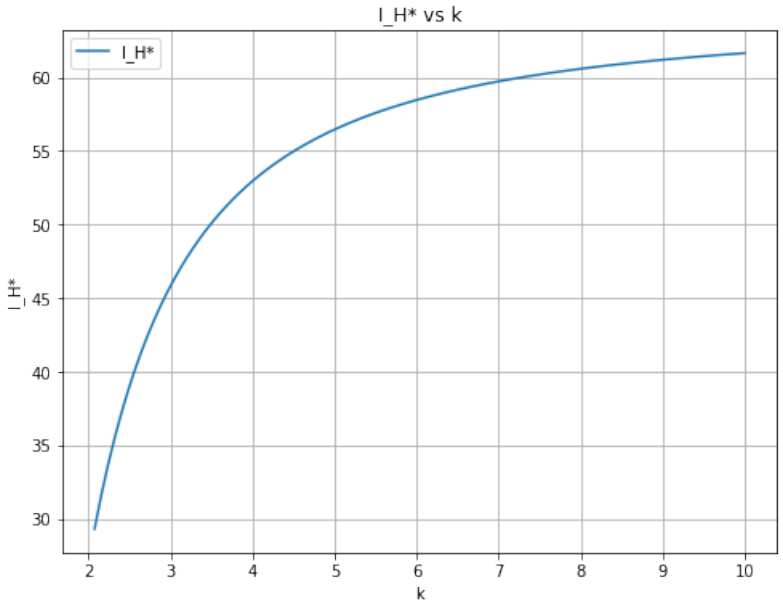


Figure 10 – $I_H^*$ given in function of $k$

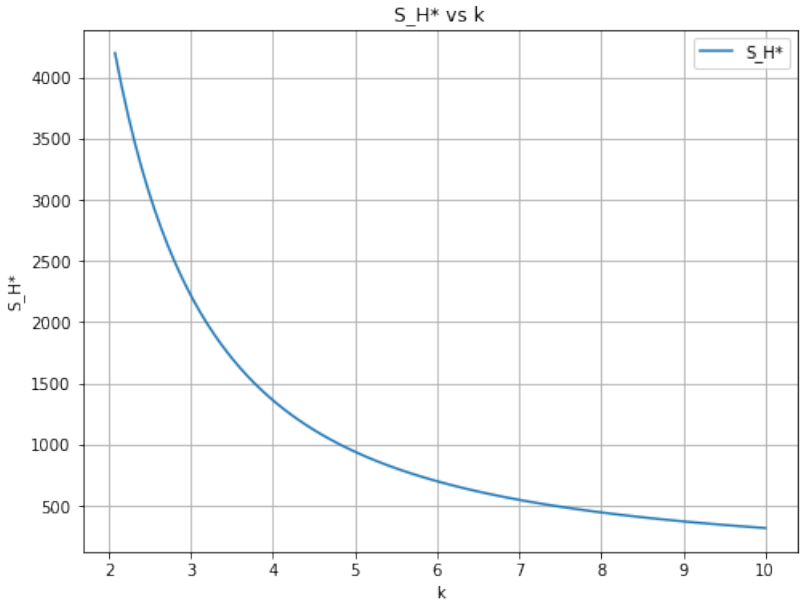


Figure 11 – $S_H^*$ given in function of $k$

By starting the plots for $k$ which makes $\mathcal{R}_0 = 1$ and for $t = 1825$, as we want the final equilibrium, it is possible to see that the endemic equilibrium of infected humans approaches to a little over 60 as $k$ increases to 10. In fact, when $k = 10$, $I_H^* \approx 61.64$. Analyzing the susceptible population, it decreases to values under 500, $S_H^* \approx 317$ when $k = 10$ [11].

We can also verify how the equilibriums between $S_H$ and $I_H$ are affected as the initial conditions vary:

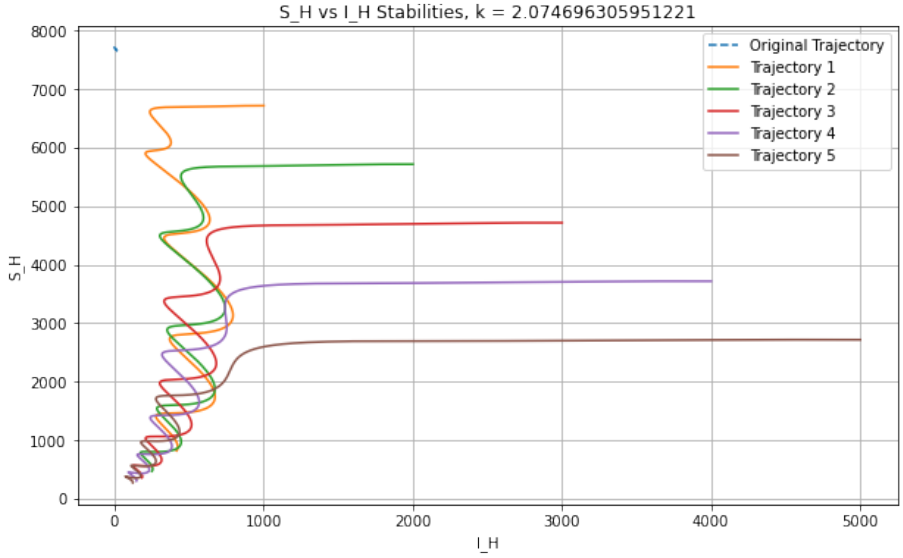


Figure 12 – Global equilibrium $S_H^* \times I_H^*$ for $k = 2.0746963059512207$

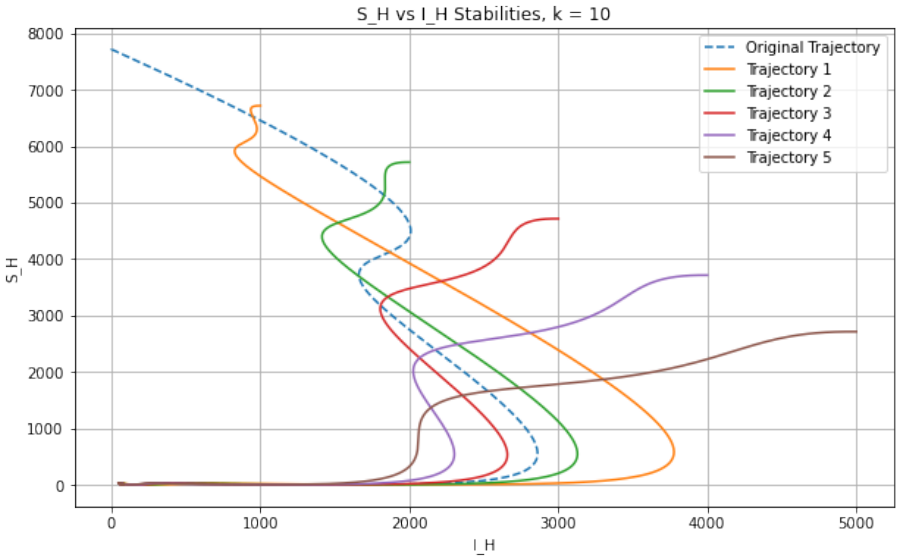


Figure 13 – Global equilibrium $S_H^* \times I_H^*$ for $k = 10$

[11] These results can be found respectively at https://github.com/RaphaLevy/Undergraduate_Dissertation/blob/main/modeling_files/Plotting_Equilibriums.ipynb.

The plottings of these populations, increasing $I_{H0}$, given in function of $t$, can be found in Appendices 43 to 46.

With this, it is possible to see that, when $\mathcal{R}_0 = 1$, the equilibrium is very close to the initial values when $I_{H0}$ is small, however, as $I_{H0}$ increases, the populations tend to become stable at values closer to $(0, 0)$. It can also be seen that the curves tend to oscilate more and more as they approach this stability.

By increasing the value of $\mathcal{R}_0$, it can be seen that even with a single initially infected human, this stability also approaches $(0, 0)$. Increasing $I_{H0}$, this behaviour is the same, getting even closer to $(0, 0)$, while oscilating less than for a smaller value of $k$.

With this, we could compare the obtained result with the calculation of the endemic equilibrium by Adda and Bichara (ADDA; BICHARA, 2011), where

$$S_H^* = \frac{1}{\mathcal{R}_0}$$
$$I_H^* = \frac{\mu_H}{\mu_H + \gamma}(1 - \frac{1}{\mathcal{R}_0})$$

Through this calculation, the population of susceptibles and infected at equilibrium was approximately 1601 and 51, respectively. Remarkably, these values deviate from those obtained through numerical calculation. However, it is necessary to consider the main difference between the proposed equations for $S$ and $I$ in this work and in the paper by Adda and Bichara, which is the use of $I_M$ in the infection rate $\beta$, given the dynamics of the coupled SEIR model in this case, which is not considered in the work of Adda and Bichara.

# 4 Discussion

Throughout the work, a SIR/SEI transmission model for malaria was developed and analyzed to complement the original methodology by Parham & Michael. The model incorporated epidemiological factors of disease transmission and complemented them with human demographic dynamics and external environmental factors such as temperature and precipitation, including deforestation, considered in the multiplicative factor for the infection-causing bite proportions.

Given the significant focus on modeling transmission and analyzing the environmental impacts, requiring various adaptations to make it more realistic and compatible with disease dynamics in the environment, the in-depth analysis of the effects of socioeconomic factors, as well as the identification of disease prevention and control strategies, ended up beyond the scope of the undergraduate thesis.

Regarding what was accomplished, a key takeaway from the work is that this model is highly sensitive to the parameters used. Small modifications are sufficient for the model to reach equilibrium or for populations to tend toward $\pm\infty$.

Indeed, what was particularly noted when modifying parameters $A$, $B$, and $C$ was that using the values indicated in the works of Parham & Michael (PARHAM; MICHAEL, 2010) and Eikenberry & Gummel (OKUNEYE; GUMEL, 2017), in the case $A = -0.03$, $B = 1.31$, $C = -4.4$, no epidemic occurred. Starting the modeling with the other parameters used in Figure 7, with $k = 1$, $\mathcal{R}_0 = 0.0207$, a value much lower than previously verified. Even with $k = 10$, $\mathcal{R}_0 = 0.207$, leading to mosquito population extinction in all cases and making the existence of endemic equilibrium unviable.

Another point that could be perceived was that in many cases, malaria takes a long time to reach endemic equilibrium. Therefore, although it was not possible to study the application of disease control strategies, it can be concluded that long-term measures may not be as effective, as the environmental conditions present at the beginning of this analysis would no longer be the same when the measure is applied.

As future work, it would be possible to compare the general methodology used by the referenced authors with the methodology used in this work and identify what could be modified so that, using the original parameters, the model still reaches endemic equilibrium.

Furthermore, as verified in the equilibrium calculations, something else that could be

studied as a continuation of the work is the analysis of its evolution over time since they are given by oscillatory functions, such as the biting rate, birth rate, mortality rate, survival probability, and the infection rate of exposed individuals, which vary depending on temperature and precipitation factors, as presented previously.

Another possible option would be to analyze the use of $k$ in relation to other parameters instead of only the infection rate, such as the mosquito's birth and mortality rates, daily survival rates, among others.

# 5 Conclusion

Throughout the development of the undergraduate thesis, different modifications to the dynamics of malaria transmission in the Amazon were explored in order to align the modeling more closely with the natural history of the disease in this environment. The ultimate goal was to understand how ecological impacts in the region affect interactions between the vector and the host.

With the obtained results, it was possible to perceive the effect that increased contact between humans and mosquitoes due to deforestation can have on malaria dynamics, based on the proportion of bites causing infection. Furthermore, it was observed how, depending on the original parameters provided, a much higher proximity between vector and host would be required for the disease to become endemic in the Amazon region. As verified, this contact could be double the normal amount, and yet it is still insufficient for the disease to become an epidemic.

To further align the methods used with observed behaviors in reality, the application of a stochastic transmission model, incorporating constantly changing environmental variables, could be ideal. However, for the proposed purpose, the deterministic model used was sufficient to highlight the disease's sensitivity to climate and environmental changes, allowing a clear and focused analysis of interactions between vector and host. This provides a solid foundation for investigating the implications of environmental changes on malaria transmission and for future research and improvements in the model.

# References


ADDA, Phillipe; BICHARA, Derdei. **Global stability for SIR and SIRS models with differential mortality**. [S.l.: s.n.], 2011. arXiv: 1112.2662 [q-bio.PE].

BACAËR, Nicolas. Ross and malaria (1911). In: A Short History of Mathematical Population Dynamics. London: Springer London, 2011. P. 65–69. ISBN 978-0-85729-115-8. DOI: 10.1007/978-0-85729-115-8_12. Available from: <https://doi.org/10.1007/978-0-85729-115-8_12>.

CLIMATEDATA.ORG. **CLIMA MANAUS (BRASIL)**. [S.l.: s.n.]. https://pt.climate-data.org/america-do-sul/brasil/amazonas/manaus-1882/.

CODEÇO, Claudia T. et al. Epidemiology, Biodiversity, and Technological Trajectories in the Brazilian Amazon: From Malaria to COVID-19. **Frontiers in Public Health**, v. 9, 2021. ISSN 2296-2565. DOI: 10.3389/fpubh.2021.647754. Available from: <https://www.frontiersin.org/articles/10.3389/fpubh.2021.647754>.

COELHO, F. C. **Github Modelagem-Matematica-IV**. [S.l.: s.n.]. https://github.com/fccoelho/Modelagem-Matematica-IV/tree/master.

DETINOVA, Tatiana Sergeevna; BERTRAM, D. S; ORGANIZATION, World Health. **Age-grouping methods in diptera of medical importance, with special reference to some vectors of malaria / T. S. Detinova ; [with] an Annex on the ovary and ovarioles of mosquitos (with glossary) by D. S. Bertram**. [S.l.]: World Health Organization, 1962. 216 p. (World Health Organization monograph series ; no. 47).

IBGE. **Censo - Séries históricas. Brasil / Amazonas / Manaus**. [S.l.: s.n.]. https://cidades.ibge.gov.br/brasil/am/manaus/pesquisa/43/0?tipo=grafico.

JOSLING, Gabrielle A.; WILLIAMSON, Kim C.; LLINÁS, Manuel. Regulation of Sexual Commitment and Gametocytogenesis in Malaria Parasites. **Annual Review of Microbiology**, v. 72, n. 1, p. 501–519, 2018. PMID: 29975590. DOI: 10.1146/annurev-micro-090817-062712. eprint: https://doi.org/10.1146/annurev-micro-090817-062712. Available from: <https://doi.org/10.1146/annurev-micro-090817-062712>.

MCCORD, G.C. Malaria ecology and climate change. **The European Physical Journal Special Topics**, v. 225, n. 3, p. 459–470, May 2016. ISSN 1951-6401. DOI: 10.1140/epjst/e2015-50097-1. Available from: <https://doi.org/10.1140/epjst/e2015-50097-1>.

NORRIS, Douglas E. Mosquito-borne Diseases as a Consequence of Land Use Change. **EcoHealth**, v. 1, n. 1, p. 19–24, Mar. 2004. ISSN 1612-9210. DOI: 10.1007/s10393-004-0008-7. Available from: <https://doi.org/10.1007/s10393-004-0008-7>.

OKUNEYE, Kamaldeen; GUMEL, Abba B. Analysis of a temperature- and rainfall-dependent model for malaria transmission dynamics. **Mathematical Biosciences**, v. 287, p. 72–92, 2017. 50th Anniversary Issue. ISSN 0025-5564. DOI: https://doi.org/10.1016/j.mbs.2016.03.013. Available from: <https://www.sciencedirect.com/science/article/pii/S0025556416300177>.

OLIVEIRA-FERREIRA, Joseli et al. Malaria in Brazil: an overview. **Malaria Journal**, v. 9, n. 1, p. 115, Apr. 2010. ISSN 1475-2875. DOI: 10.1186/1475-2875-9-115. Available from: <https://doi.org/10.1186/1475-2875-9-115>.

PARHAM, Paul E.; MICHAEL, Edwin. Modelling Climate Change and Malaria Transmission. In: **Modelling Parasite Transmission and Control**. Ed. by Edwin Michael and Robert C. Spear. New York, NY: Springer New York, 2010. P. 184–199. ISBN 978-1-4419-6064-1. DOI: 10.1007/978-1-4419-6064-1_13. Available from: <https://doi.org/10.1007/978-1-4419-6064-1_13>.

PIMENTA, Paulo FP et al. An overview of malaria transmission from the perspective of Amazon *Anopheles vectors*. **Memórias do Instituto Oswaldo Cruz**, Instituto Oswaldo Cruz, Ministério da Saúde, v. 110, n. 1, p. 23–47, Feb. 2015. ISSN 0074-0276. DOI: 10.1590/0074-02760140266. Available from: <https://doi.org/10.1590/0074-02760140266>.

PRASAD, Ramakant et al. Mathematical modeling in perspective of vector-borne viral infections: a review. **Beni-Suef University Journal of Basic and Applied Sciences**, v. 11, n. 1, p. 102, Aug. 2022. ISSN 2314-8543. DOI: 10.1186/s43088-022-00282-4. Available from: <https://doi.org/10.1186/s43088-022-00282-4>.

RONDÔNIA, Fiocruz. **Anopheles**. [S.l.: s.n.]. https://www.rondonia.fiocruz.br/pivem/anopheline/.

RORATO, Ana C. et al. Trajetorias: a dataset of environmental, epidemiological, and economic indicators for the Brazilian Amazon. **Scientific Data**, v. 10, n. 1, p. 65, Feb. 2023. ISSN 2052-4463. DOI: 10.1038/s41597-023-01962-1. Available from: <https://doi.org/10.1038/s41597-023-01962-1>.

SILVA-NUNES, M. da et al. Malaria on the Amazonian frontier: transmission dynamics, risk factors, spatial distribution, and prospects for control. **Am J Trop Med Hyg**, v. 79, n. 4, p. 624–635, Oct. 2008.

SILVA-NUNES, Mônica. Environmental changes impact in malaria transmition and prospects for the disease control in brazilian amazon rural settlements. **Oecologia Australis**, v. 14, p. 603–622, Jan. 2010. DOI: 10.4257/oeco.2010.1403.02.

SILVA-NUNES, Mônica da et al. Amazonian malaria: Asymptomatic human reservoirs, diagnostic challenges, environmentally driven changes in mosquito vector populations, and the mandate for sustainable control strategies. **Acta Tropica**, v. 121, n. 3, p. 281–291, 2012. Tackling The Malaria "End Game": Regional Needs And Challenges For Successful Malaria Elimination. ISSN 0001-706X. DOI: https://doi.org/10.1016/j.actatropica.2011.10.001. Available from: <https://www.sciencedirect.com/science/article/pii/S0001706X11002865>.

VAN DEN DRIESSCHE, P.; WATMOUGH, James. Reproduction numbers and sub-threshold endemic equilibria for compartmental models of disease transmission. **Mathematical Biosciences**, v. 180, n. 1, p. 29–48, 2002. ISSN 0025-5564. DOI: https://doi.org/10.1016/S0025-5564(02)00108-6. Available from: <https://www.sciencedirect.com/science/article/pii/S0025556402001086>.

# Appendix

# APPENDIX A – Results

In this section, there will be included some resulting plots obtained of the development of the dissertation.

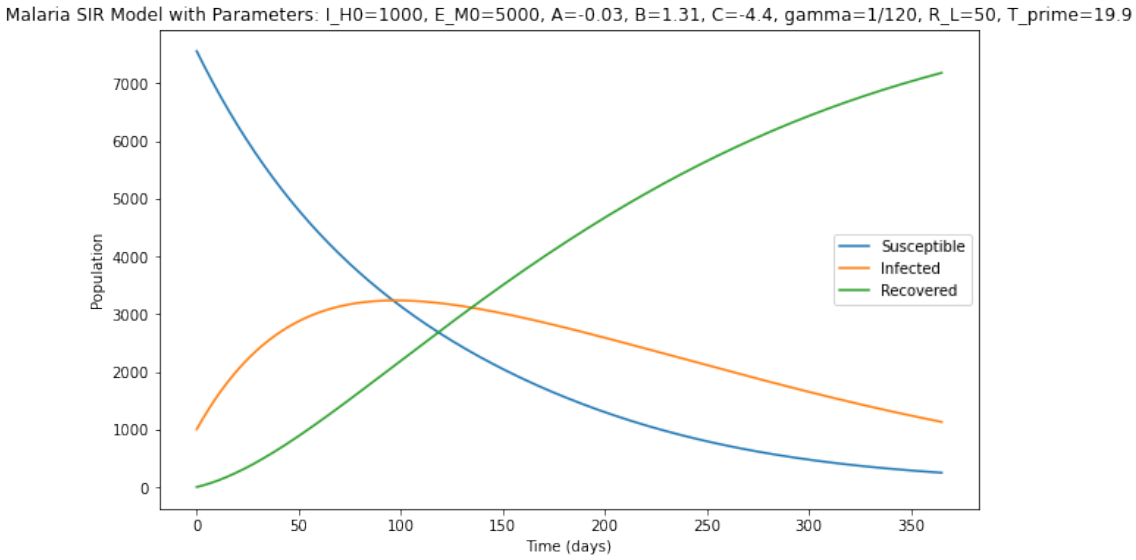


Appendix 1: SIR model with corrected $T$ and $R$

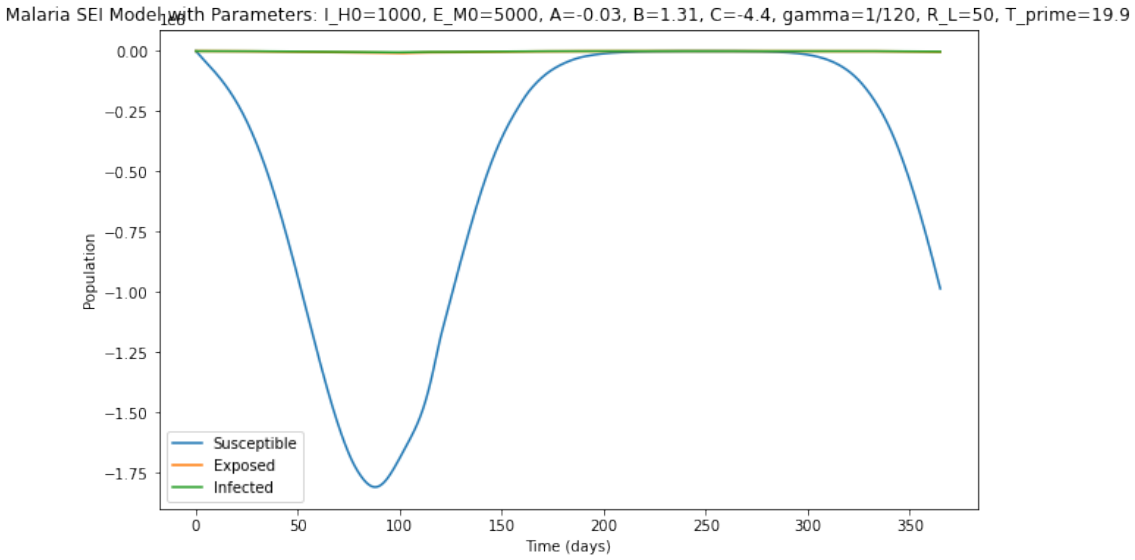


Appendix 2: SEI model with corrected $T$ and $R$

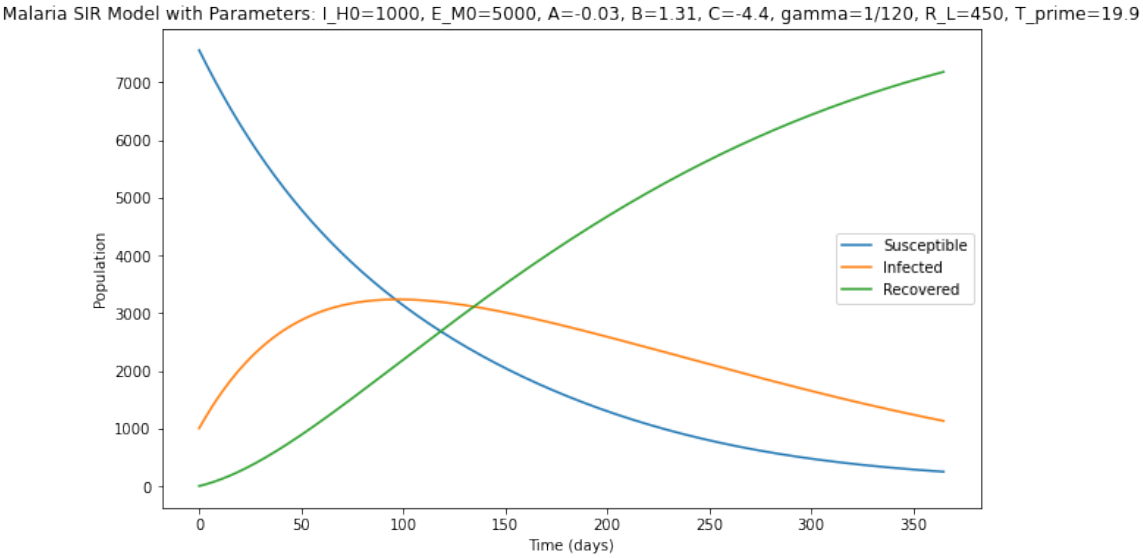


Appendix 3: SIR model with corrected $R_L$

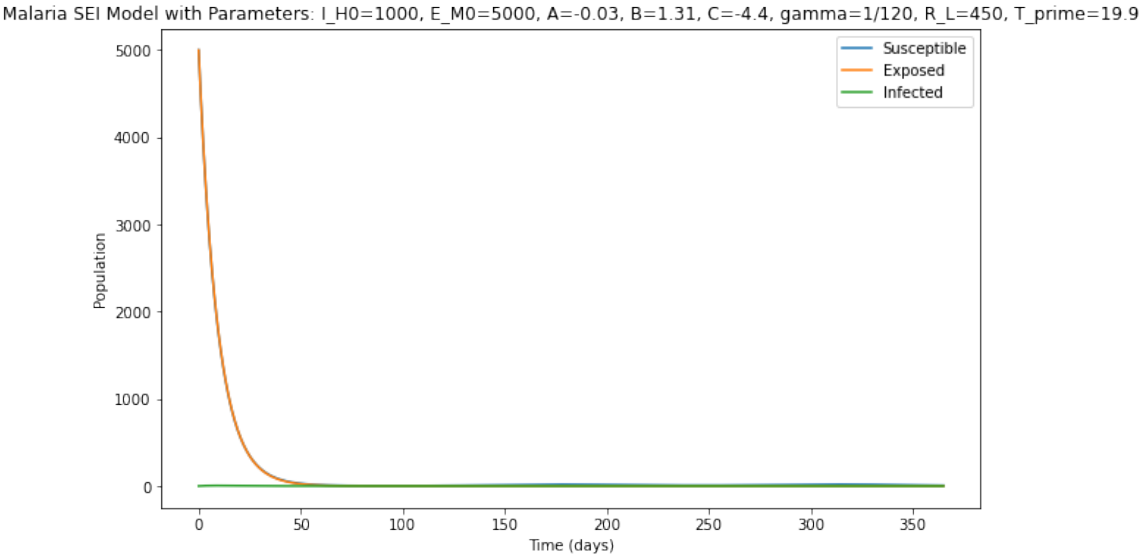


Appendix 4: SEI model with corrected $R_L$

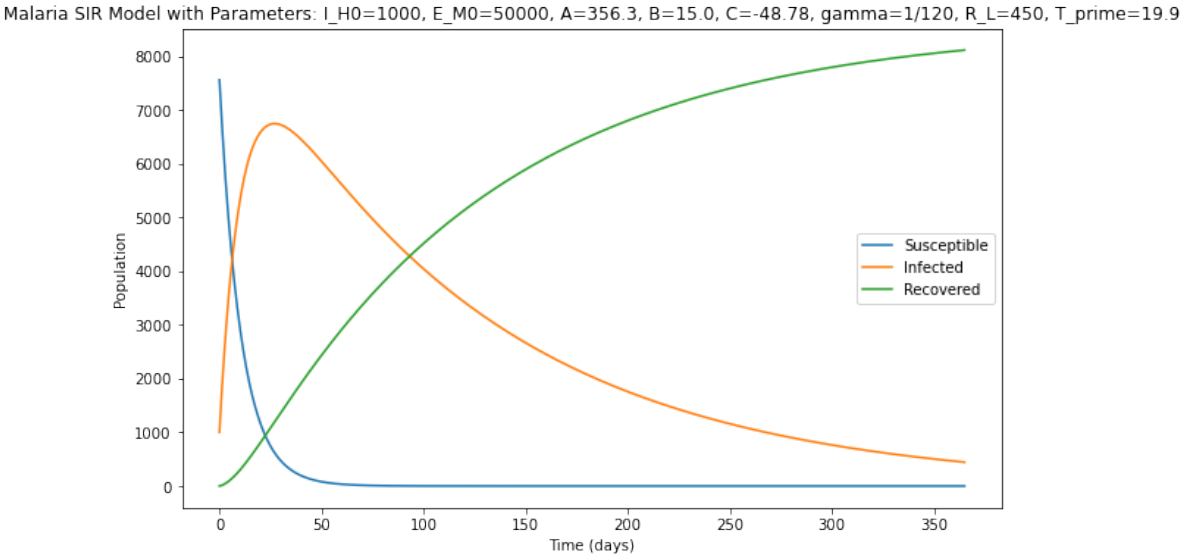


Appendix 5: SIR model with modified $A$, $B$ and $C$

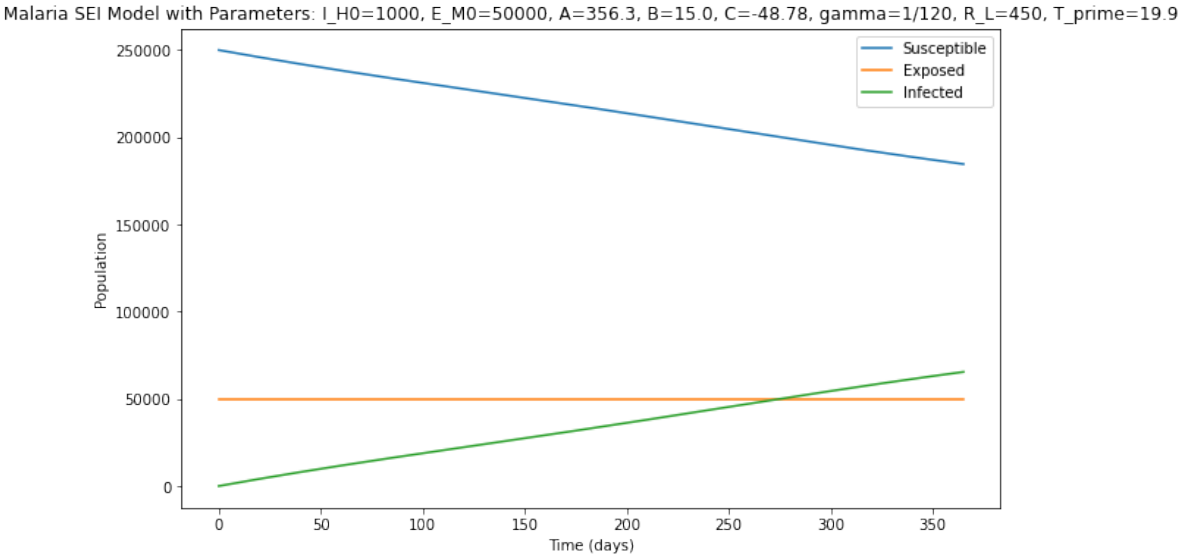


Appendix 6: SEI model with modified $A$, $B$ and $C$

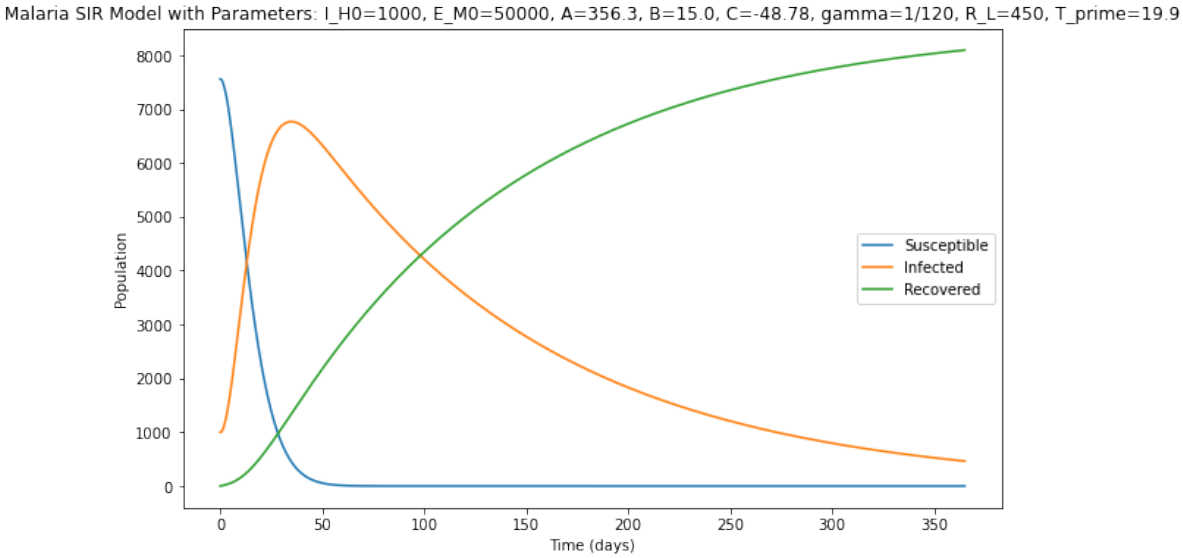


Appendix 7: SIR model with the inclusion of $b_3$ and $T' = 19.9°C$

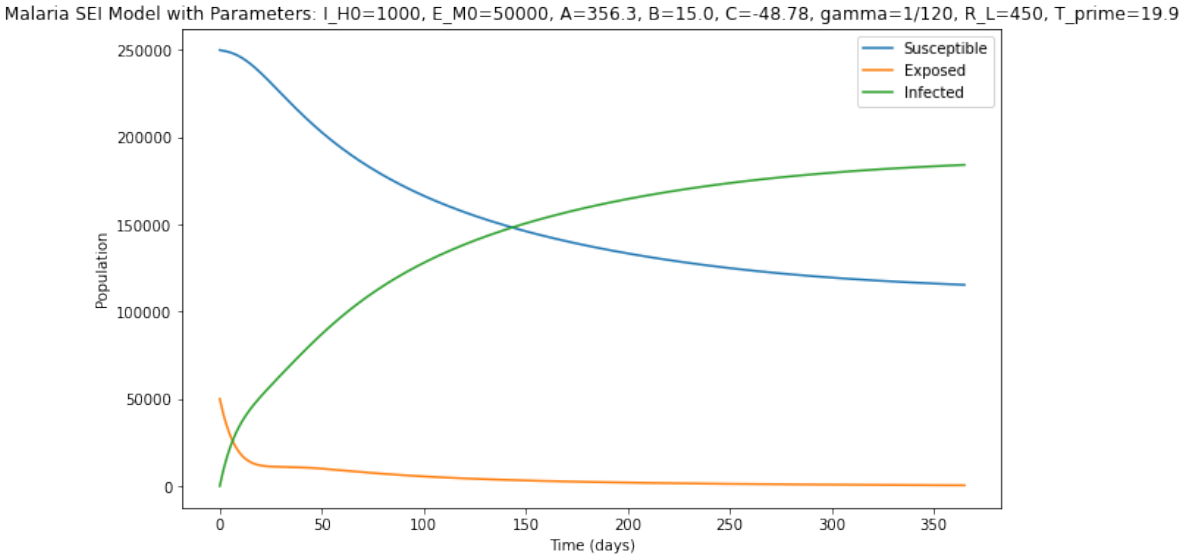


Appendix 8: SEI model with the inclusion of $b_3$ and $T' = 19.9°C$

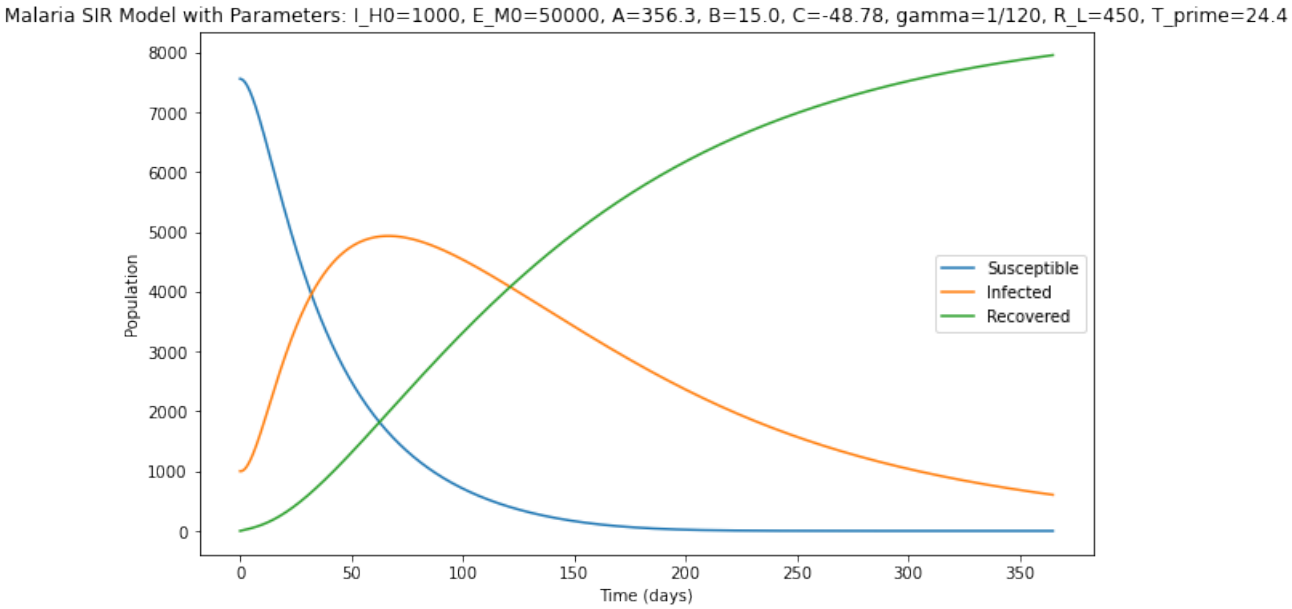


Appendix 9: SIR model with the inclusion of $b_3$ and $T' = 24.4°C$

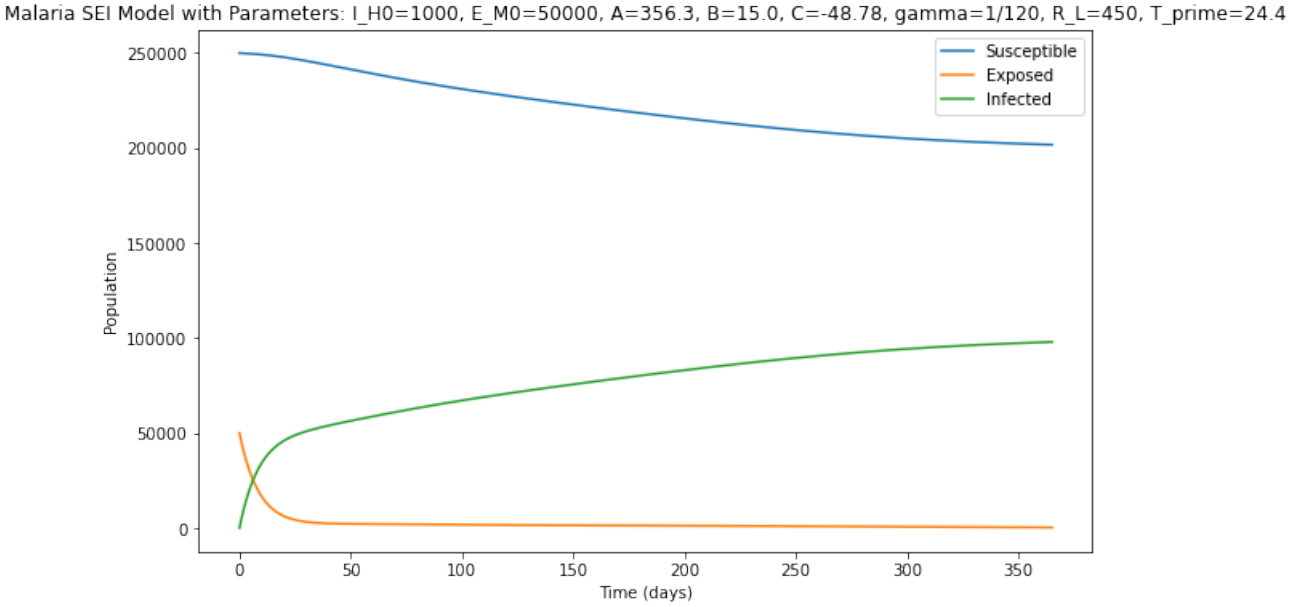


Appendix 10: SEI model with the inclusion of $b_3$ and $T' = 24.4°C$

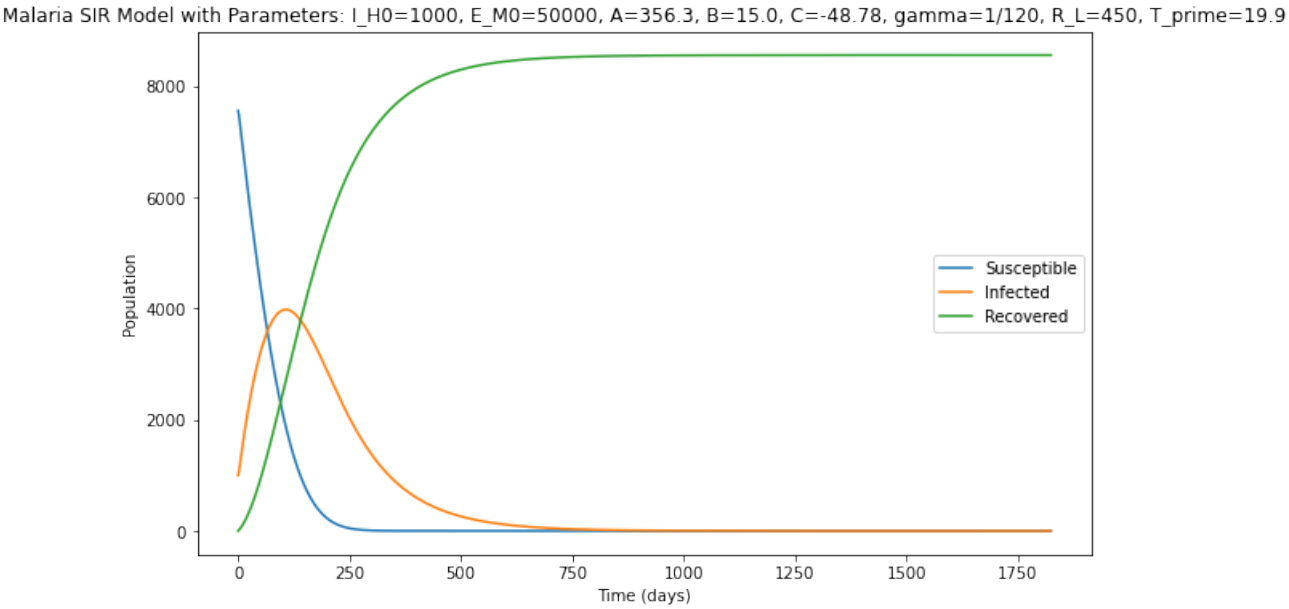


Appendix 11: SIR model modifying $l$ and $T' = 19.9°C$

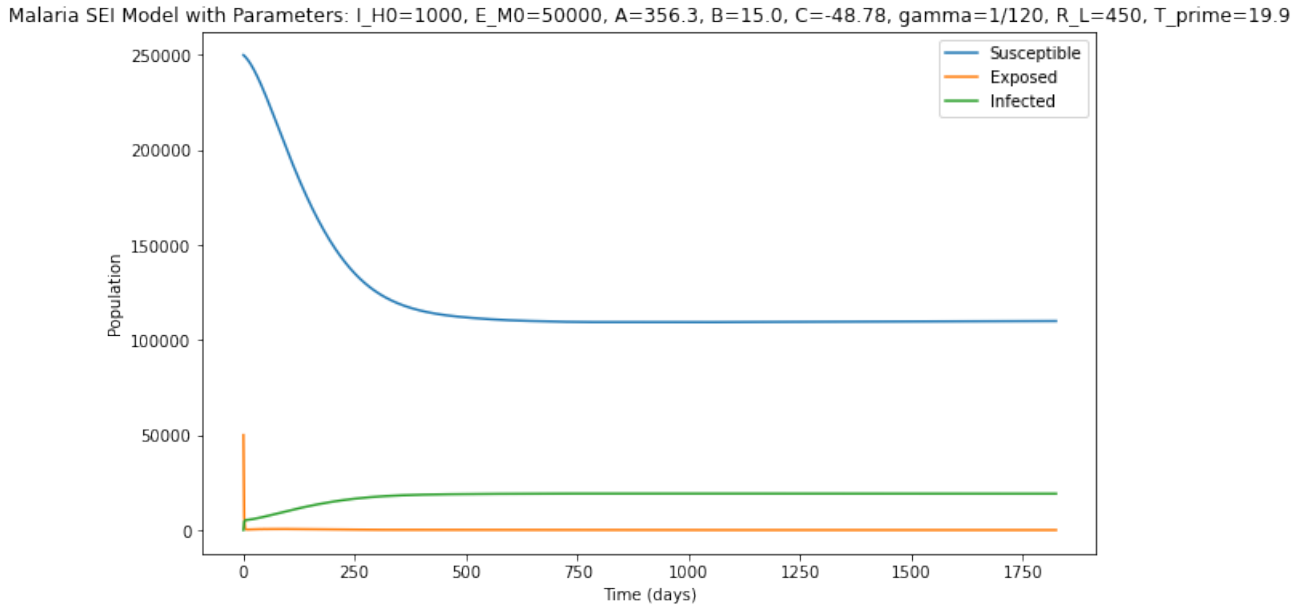


Appendix 12: SEI model modifying $l$ and $T' = 19.9°C$

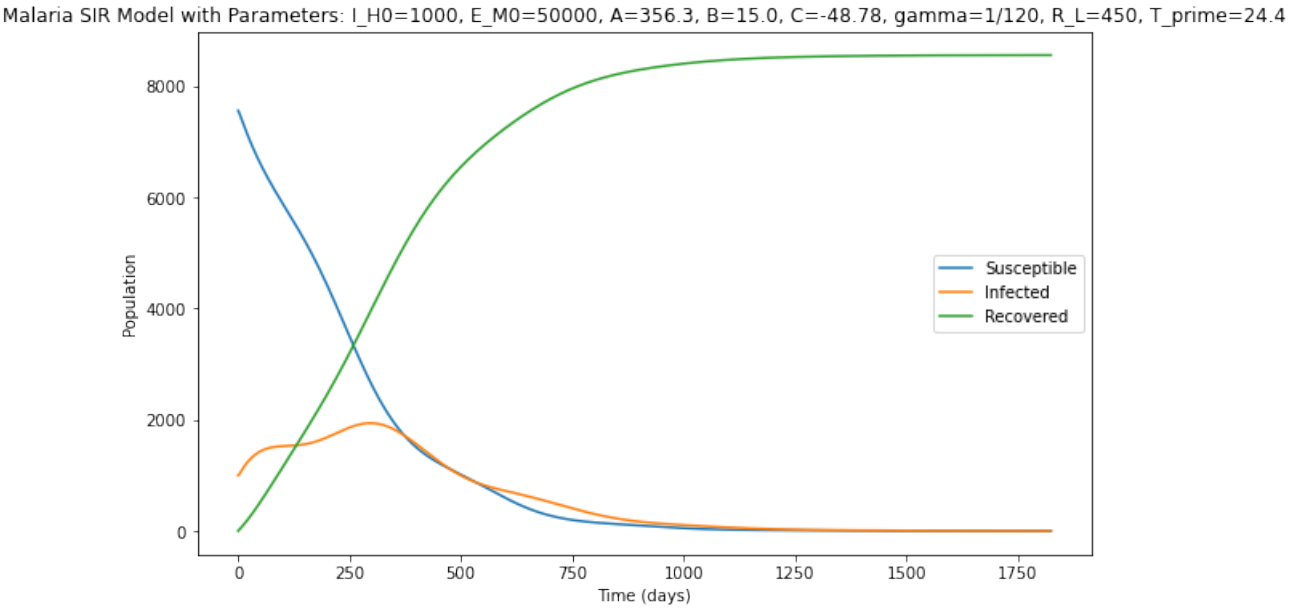


Appendix 13: SIR model modifying $l$ and $T' = 24.4°C$

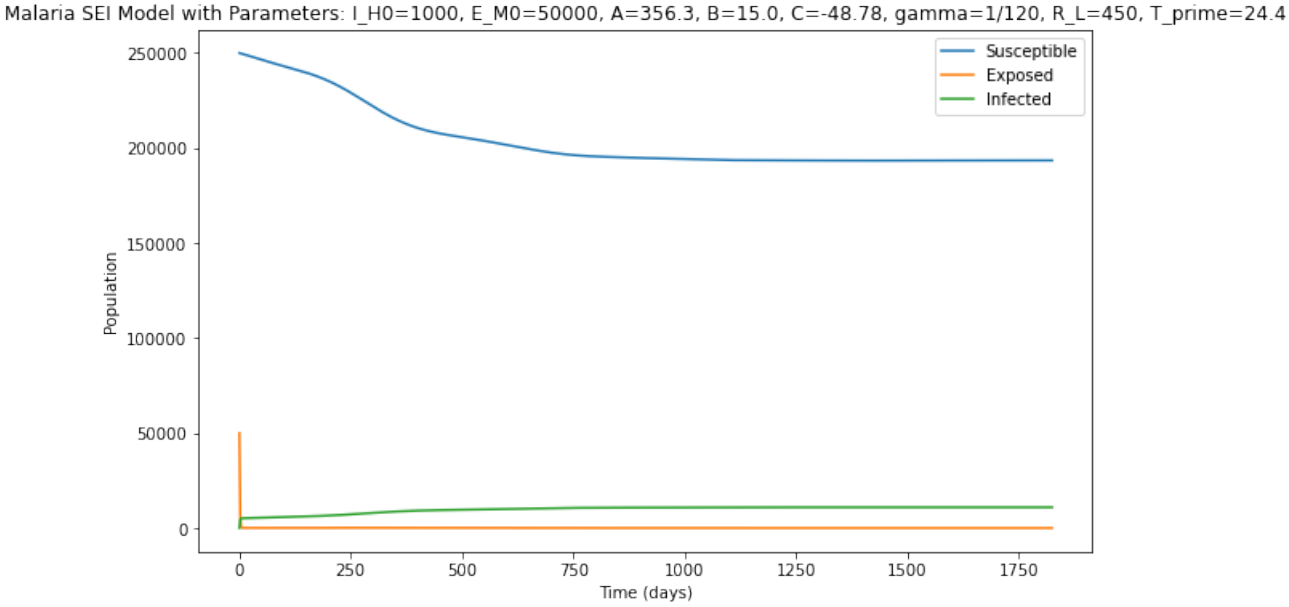


Appendix 14: SEI model modifying $l$ and $T' = 24.4°C$

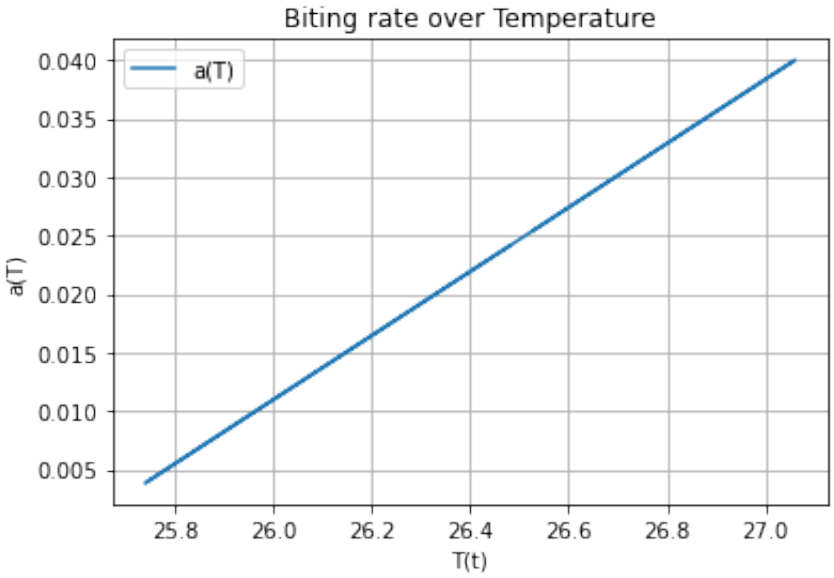


Appendix 15: Biting rate ($a(T)$)

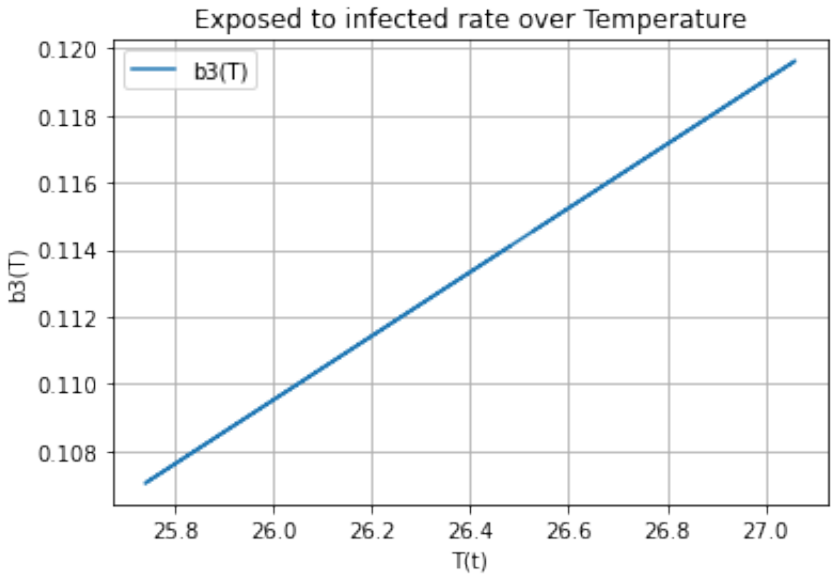


Appendix 16: Exposed to infected rate ($b_3(T)$)

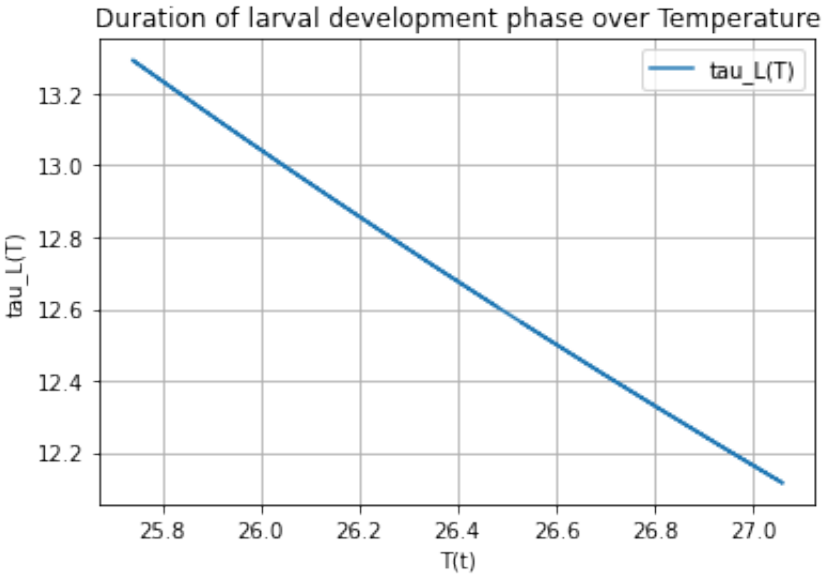


Appendix 17: Duration of larval development ($\tau_L(T)$)

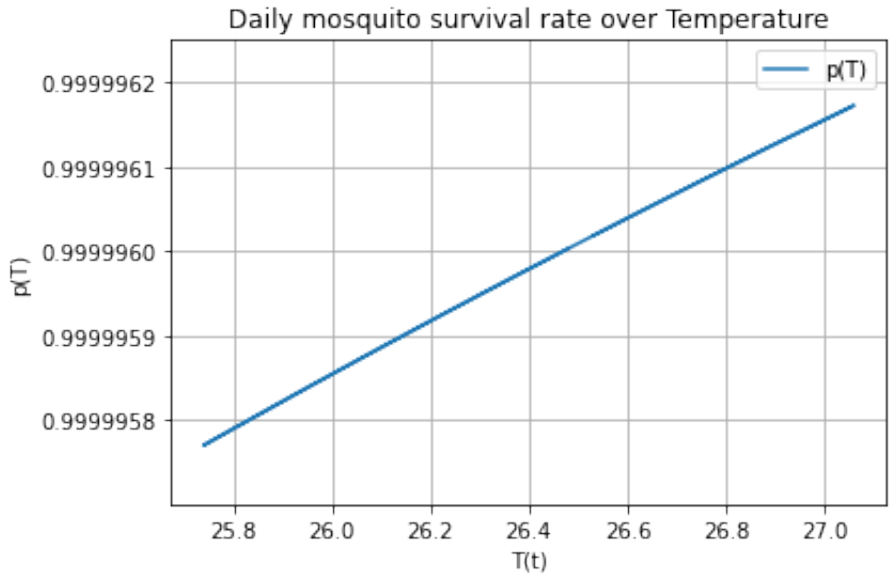


Appendix 18: Daily mosquito survival rate ($p(T)$)

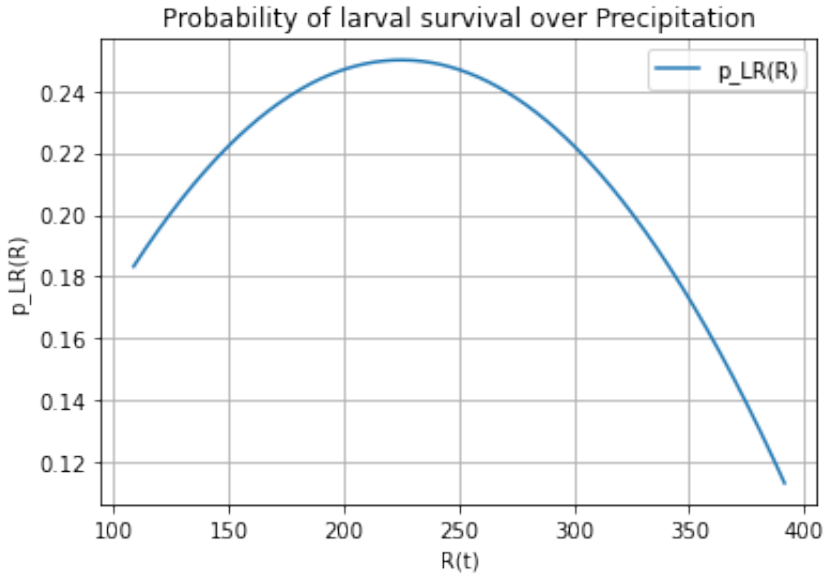


Appendix 19: Probability of larval survival ($p_{LR}(R)$)

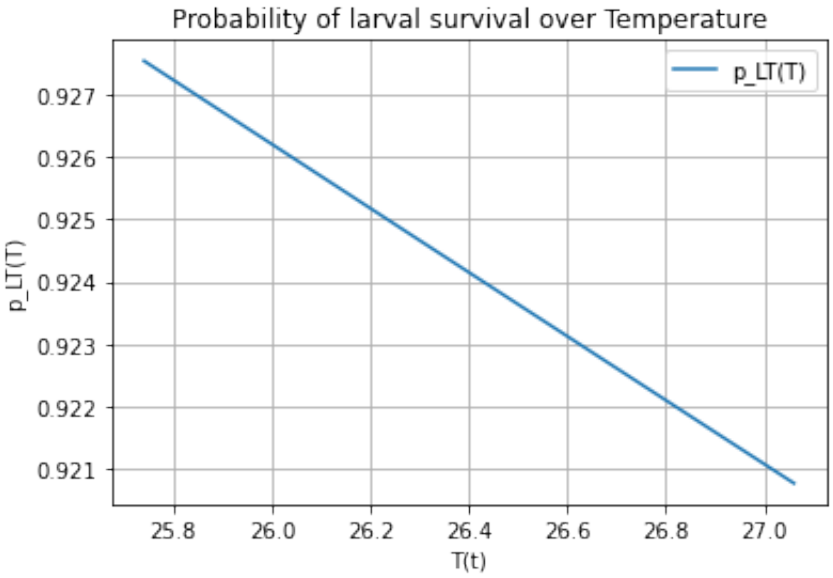


Appendix 20: Probability of larval survival ($p_{LT}(T)$)

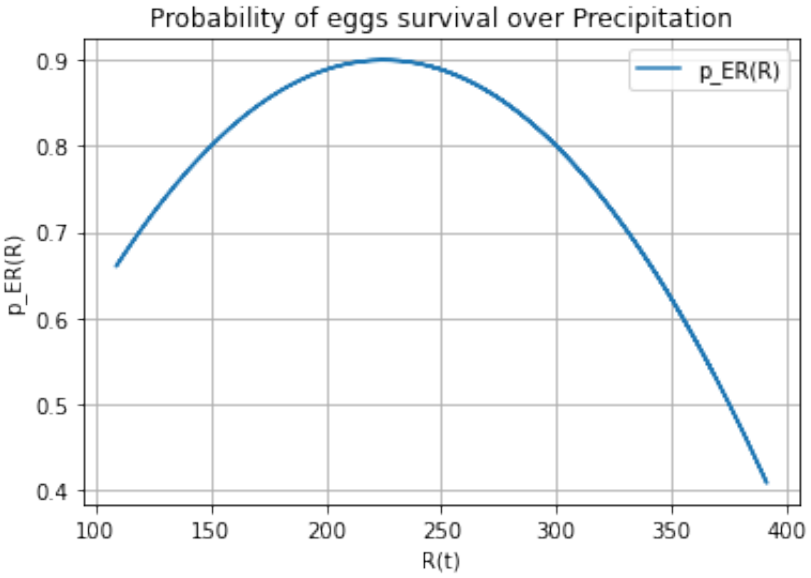


Appendix 21: Probability of larval survival ($p_{ER}(R)$)

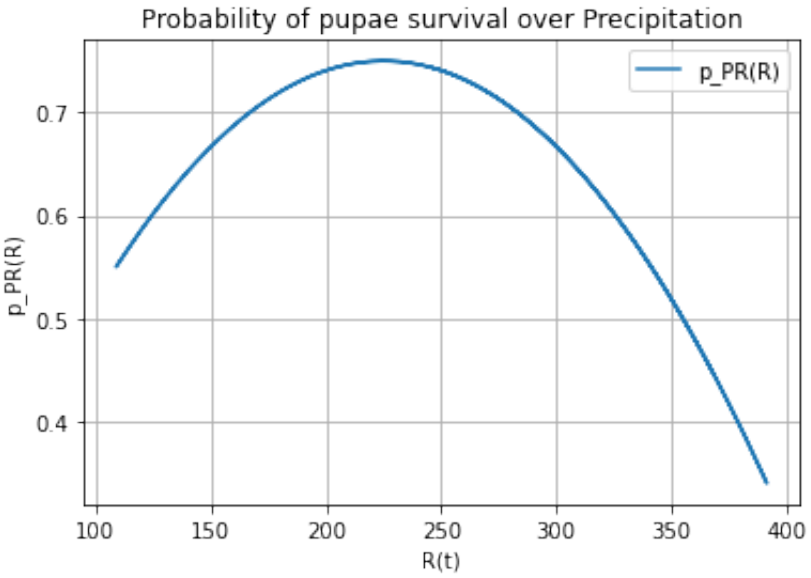


Appendix 22: Probability of larval survival ($p_{PR}(R)$)

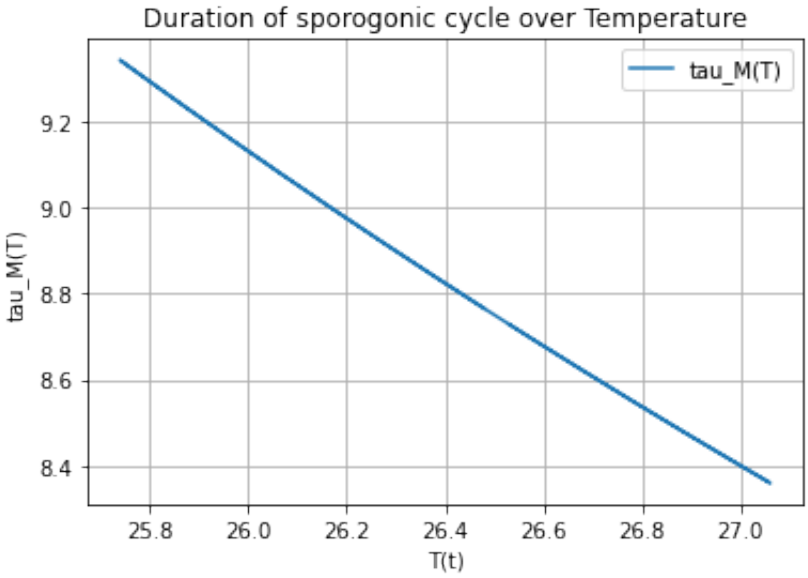


Appendix 23: Duration of sporogonic cycle ($\tau_M(T)$)

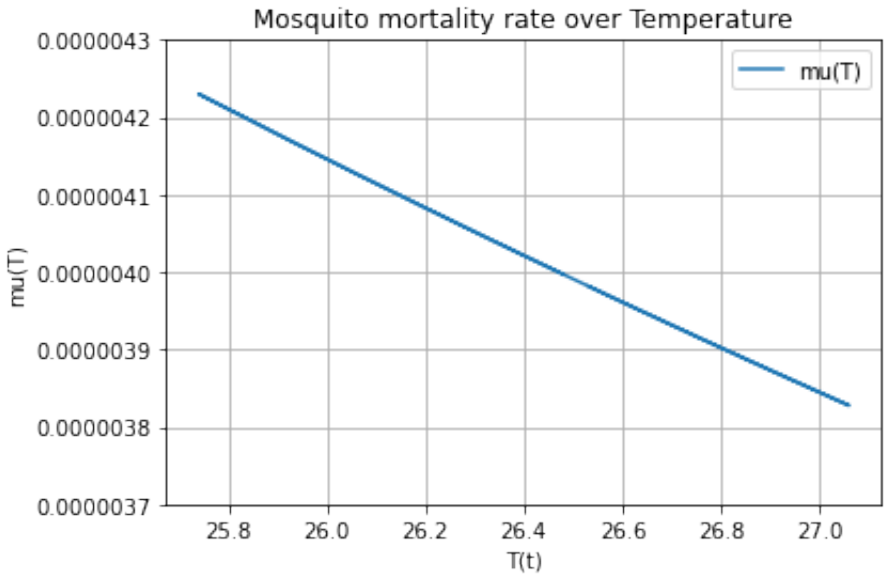


Appendix 24: Mosquito mortality rate ($\mu(T)$)

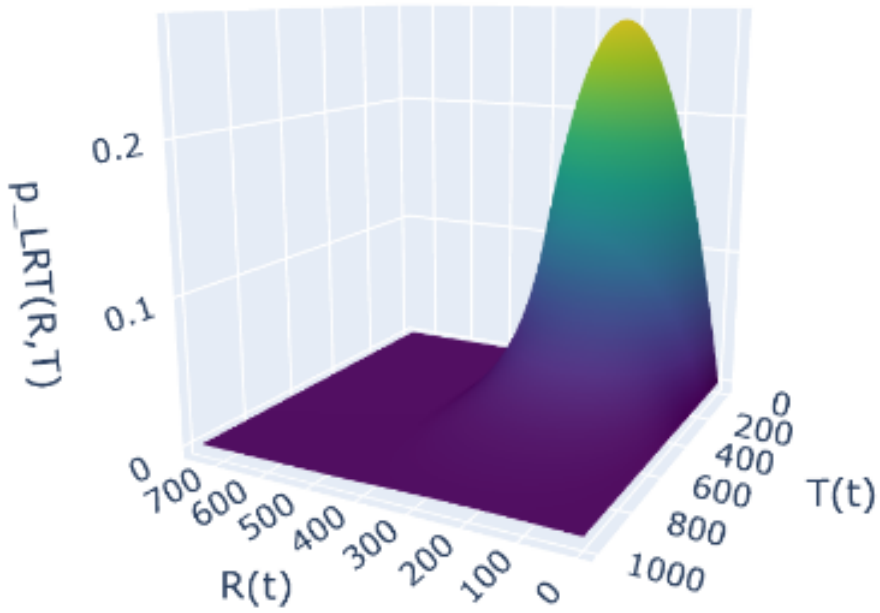


Appendix 25: Probability of larval survival ($p_{LRT}(R,T)$)

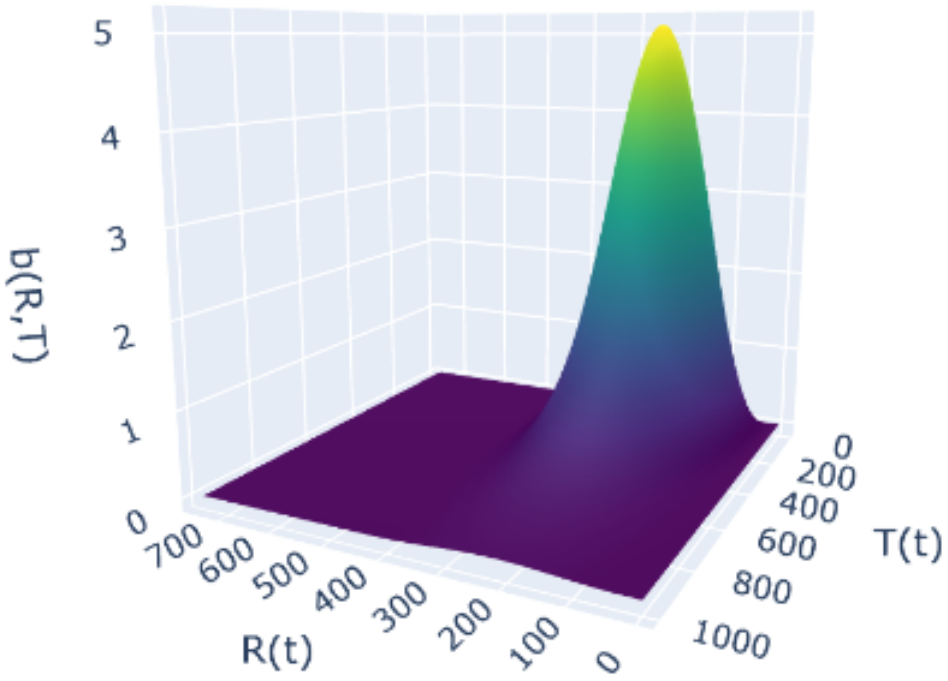


Appendix 26: Mosquito mortality rate ($b(R,T)$)

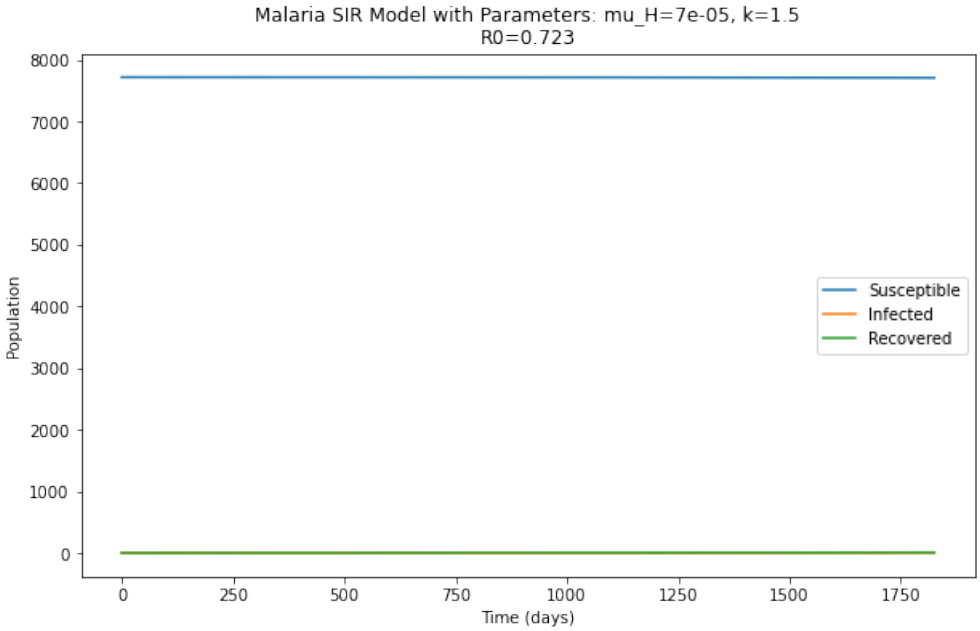


Appendix 27: SIR model with $k = 1.5$

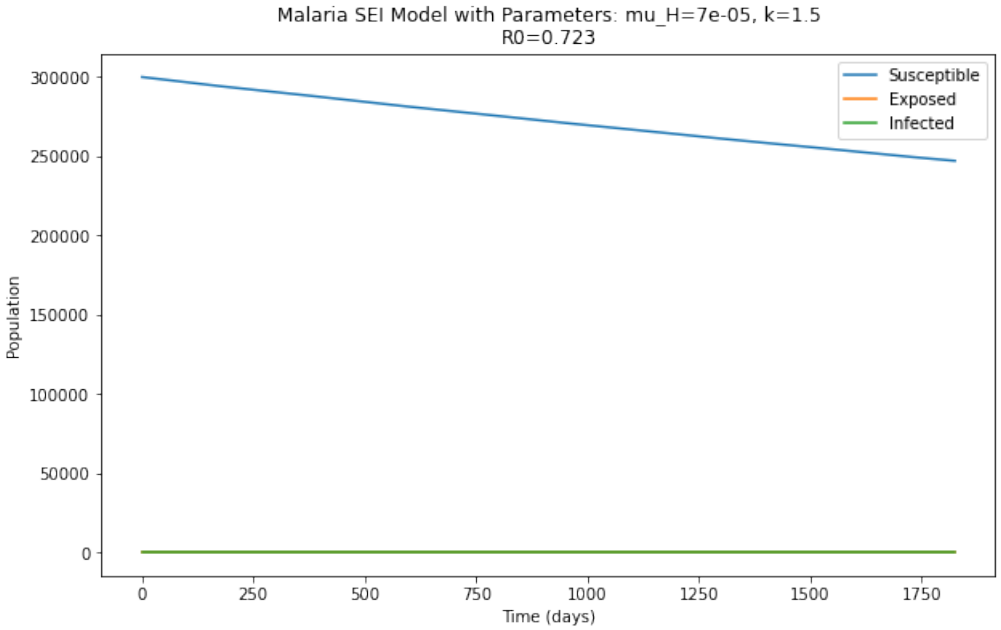


Appendix 28: SEI model with $k = 1.5$

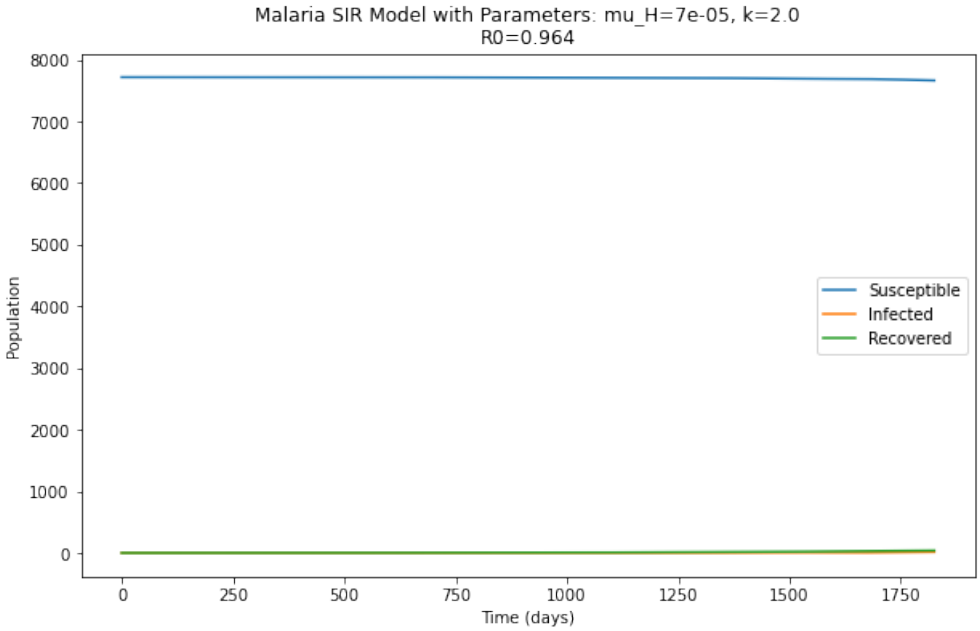


Appendix 29: SIR model with $k = 2$

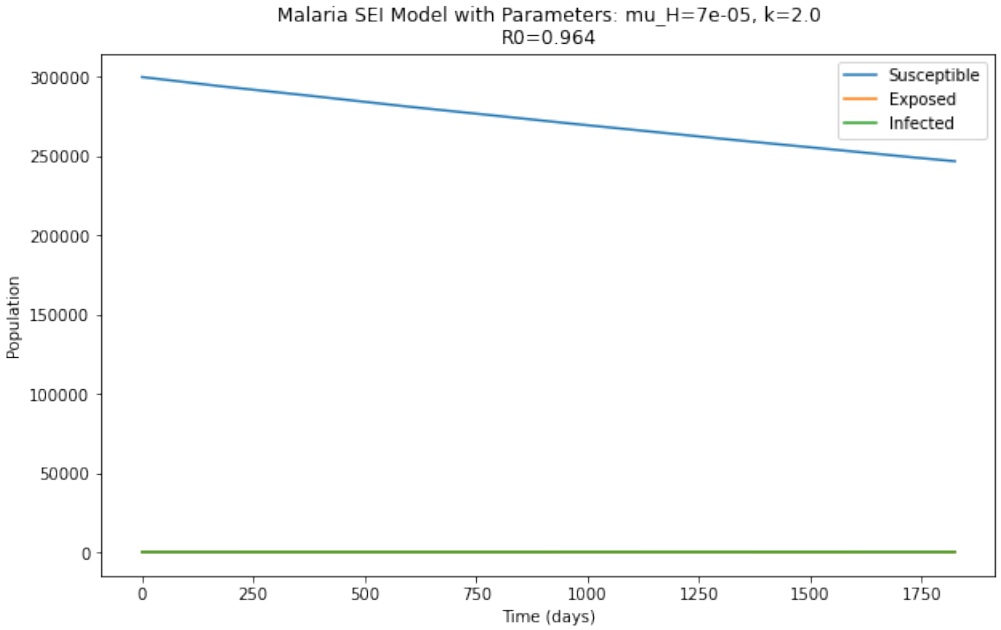


Appendix 30: SEI model with $k = 2$

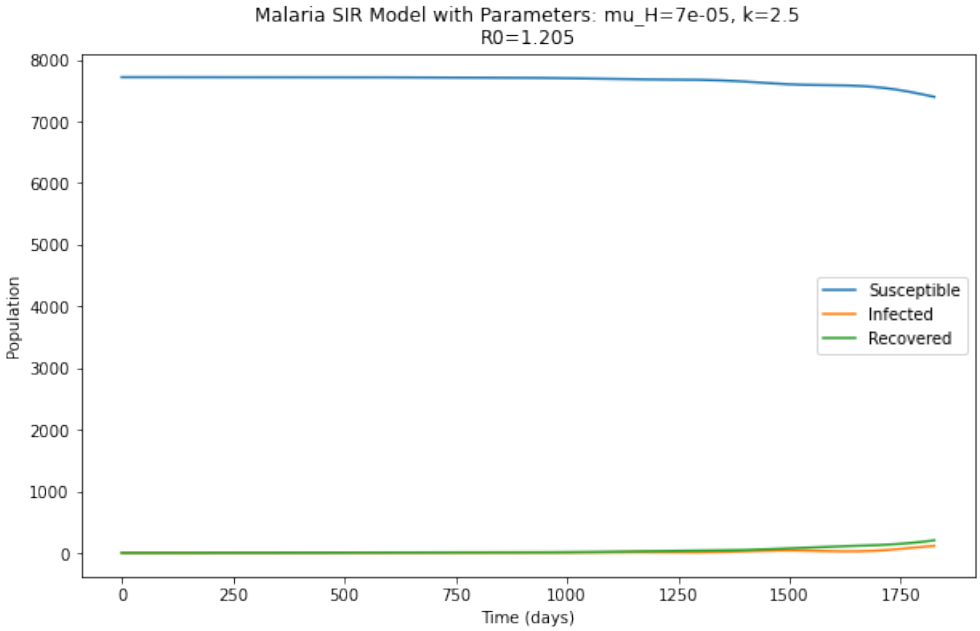


Appendix 31: SIR model with $k = 2.5$

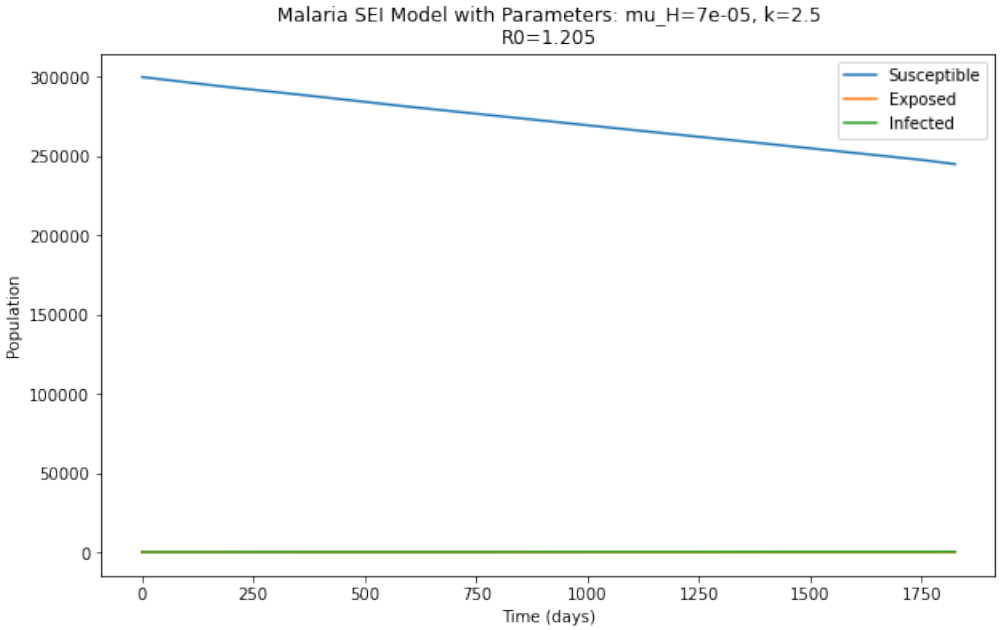


Appendix 32: SEI model with $k = 2.5$

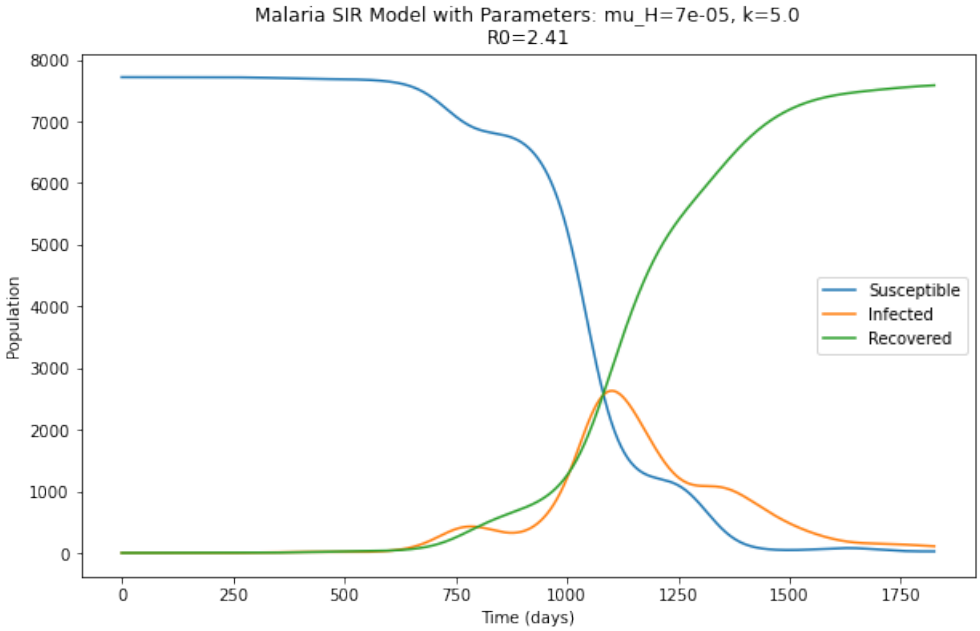


Appendix 33: SIR model with $k = 5$

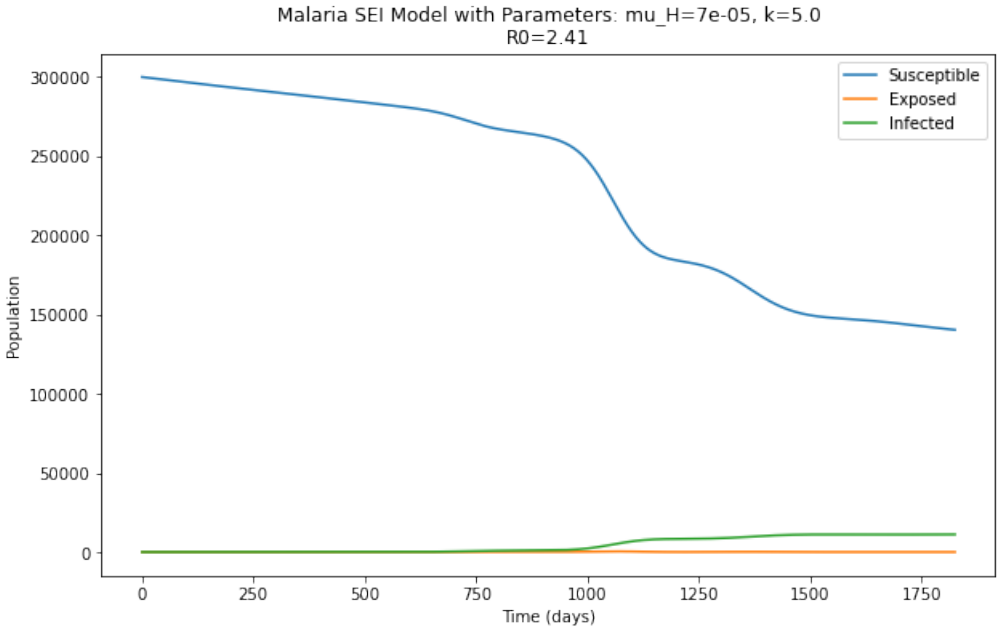


Appendix 34: SEI model with $k = 5$

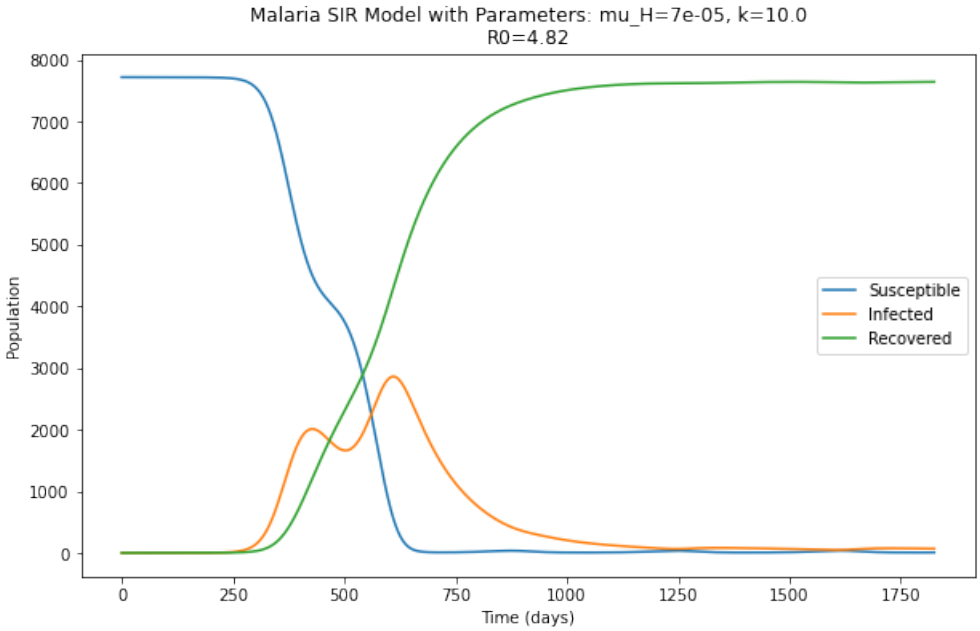


Appendix 35: SIR model with $k = 10$

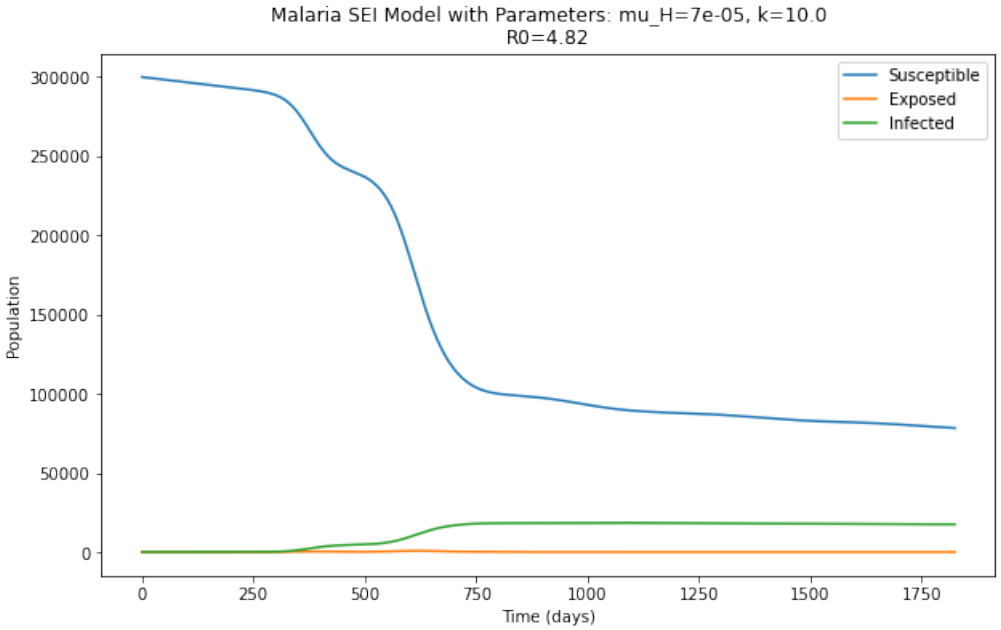


Appendix 36: SEI model with $k = 10$

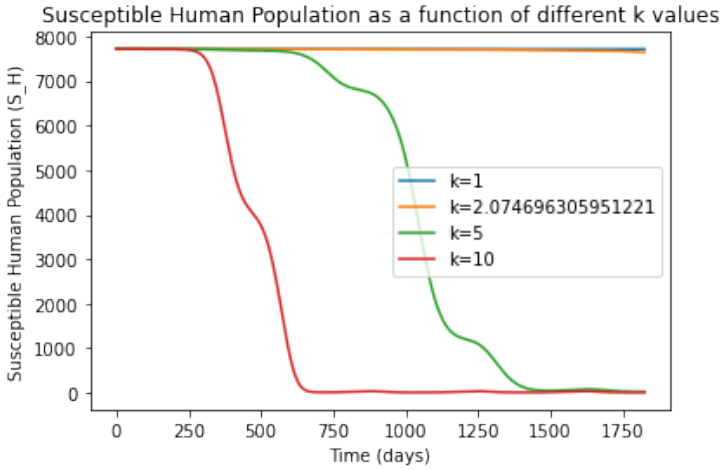


Appendix 37: Susceptible human population for varying values of $k$

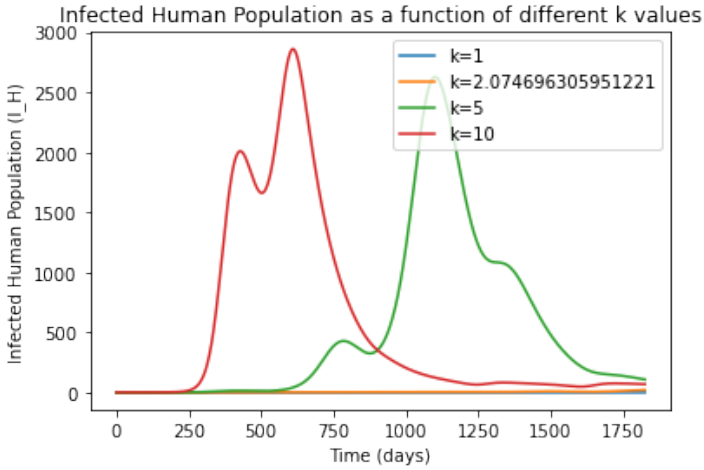


Appendix 38: Infected human population for varying values of $k$

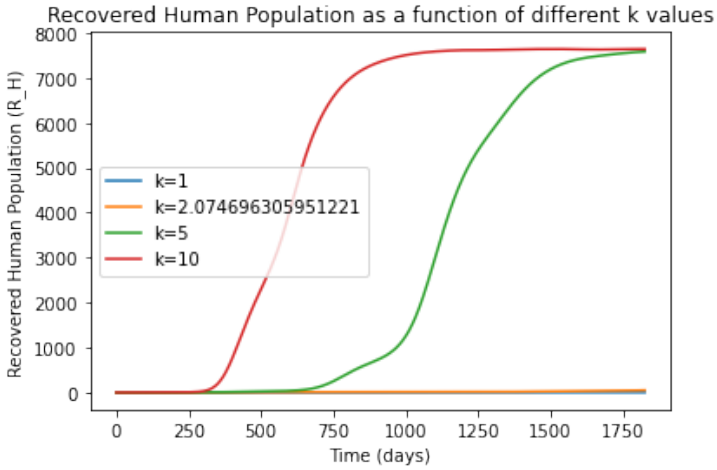


Appendix 39: Recovered human population for varying values of $k$

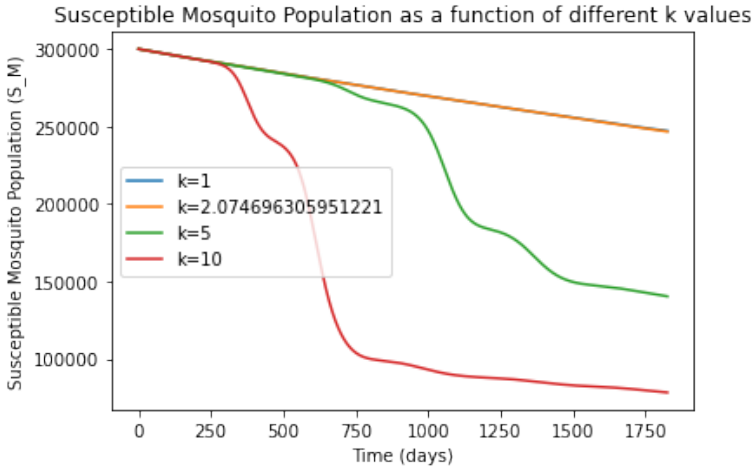


Appendix 40: Susceptible mosquito population for varying values of $k$

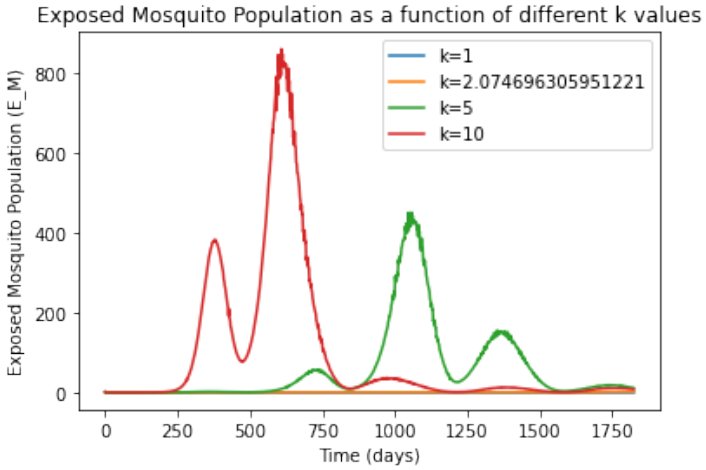


Appendix 41: Exposed mosquito population for varying values of $k$

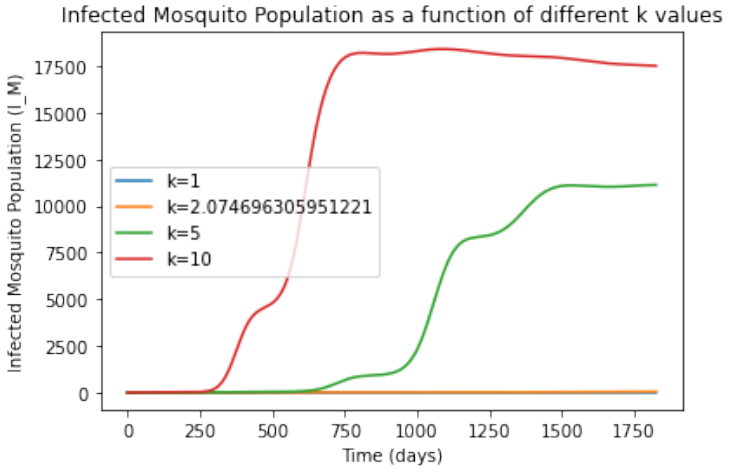


Appendix 42: Infected mosquito population for varying values of $k$

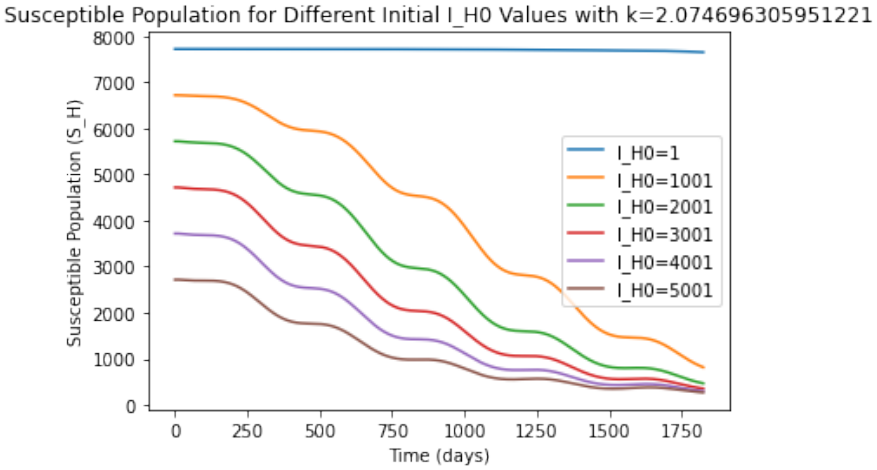


Appendix 43: Susceptible human population for varying values of $I_{H0}$, $k \approx 2.075$

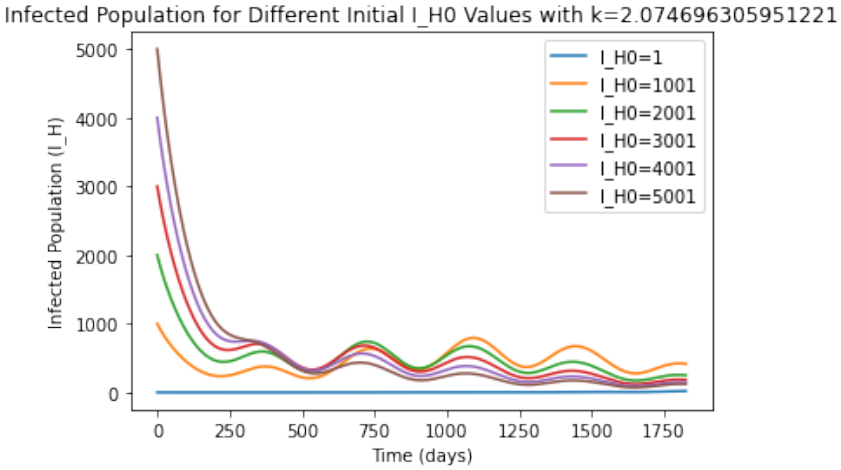


Appendix 44: Infected human population for varying values of $I_{H0}$, $k \approx 2.075$

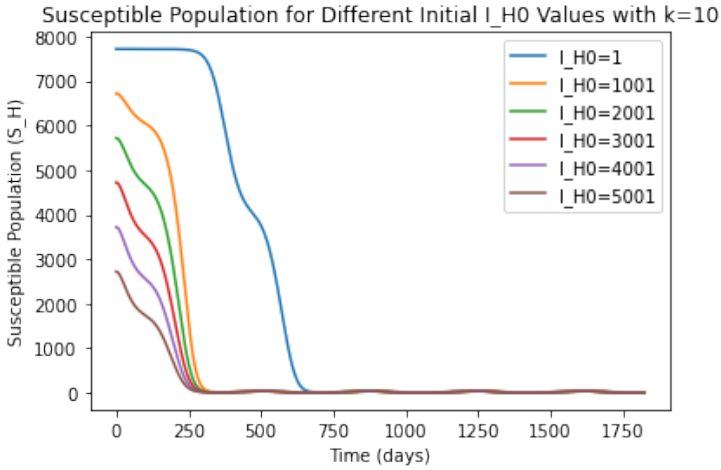


Appendix 45: Susceptible human population for varying values of $I_{H0},\ k = 10$

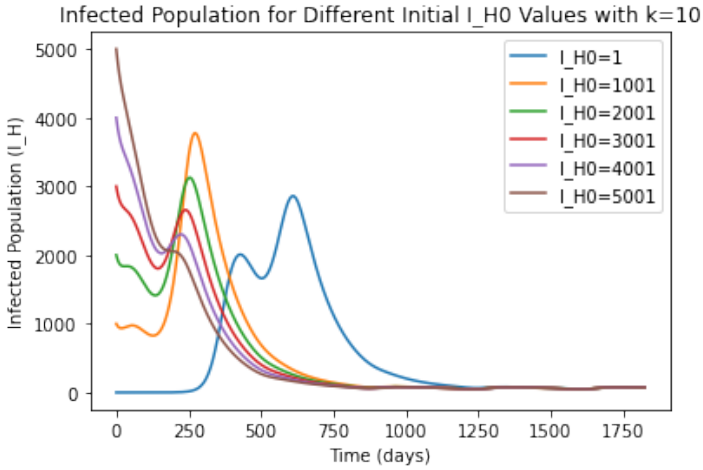


Appendix 46: Infected human population for varying values of $I_{H0},\ k = 10$